Recent Publications in this Series

2/2013 Otso Häärä
Integration of Eda Signaling with Other Signaling Pathways in Oral Ectodermal Organogenesis
3/2013 Aino Vesikansa
Developing Glutamatergic Connectivity in the Hippocampus: The Role of Tonically Active Kainate Receptors
4/2013 Petteri Heljo
Comparison of Disaccharides and Polyalcohols as Stabilizers in Freeze-Dried Protein Formulations
5/2013 Ružica Kolaković
Nanofibrillar Cellulose in Drug Delivery
6/2013 Nenad Manevski
Activity and Enzyme Kinetics of Human UDP-Glucuronosyltransferases: Studies of Psilocin Glucuronidation and the Effects of Albumin on the Enzyme Kinetic Mechanism
7/2013 Jonna Wikström
Alginate-Based Microencapsulation and Lyophilization of Human Retinal Pigment Epithelial Cell Line (ARPE-19) for Cell Therapy
8/2013 Nina S. Atanasova
Viruses and Antimicrobial Agents from Hypersaline Environments
9/2013 Tiina Rasila
Functional Mapping of Mu Transposition Machinery: MuA Protein Modification and Engineering for Hyperactivity
10/2013 Johanna Rajasärkkä
Development of High-Throughput Yeast-Cell-Based Bioreporter Assays for Specific Monitoring of Bisphenol A and Chemical Testing of Endocrine Disrupting Compounds
11/2013 Lin Ning
Neuronal Synaptic Formation Regulated by Intercellular Adhesion Molecule-5 (ICAM-5)
12/2013 Shinya Matsuda
The Extracellular Regulation of Bone Morphogenetic Proteins in Drosophila and Sawfly Wing
13/2013 Grit Kabiersch
Fungal Tools for the Degradation of Endocrine Disrupting Compounds
14/2013 Stina Parkkamäki
Voimaantumiseen pohjautuva tyypin 2 diabeteksen omahoidon tuki apteekissa — esimerkkinä Mäntyharjun Havu-apteekki
15/2013 Niina Leikoski
Cyanobactins - Ribosomally Synthesized and Post-Translationally Modified Peptides Produced by Cyanobacteria
16/2013 Hanna Sinkko
Sediment Bacterial Communities in Nutrient Cycling and in the History of the Baltic Sea
17/2013 Tuuli Haikonen
Microtubule and Replication Vesicle Associations of the Potyviral HCpro Protein
18/2013 Julia Lehtinen
In Vitro, *In Vivo*, and *In Silico* Investigations of Polymer and Lipid Based Nanocarriers for Drug and Gene Delivery
19/2013 Sirkku Jäntti
Liquid Chromatography-Tandem Mass Spectrometry in Studies of Steroid Hormones and Steroid Glucuronide Conjugates in Brain and Urine

Helsinki 2013 ISSN 1799-7372 ISBN 978-952-10-9270-1

ANU VAIKKINEN Direct Open Air Surface Sampling/Ionization MS Methods in the Study of Neutral and Nonpolar Compounds 20/2013

DISSERTATIONES BIOCENTRI VIIKKI UNIVERSITATIS HELSINGIENSIS 20/2013

ANU VAIKKINEN

Direct Open Air Surface Sampling/Ionization Mass Spectrometry Methods in the Study of Neutral and Nonpolar Compounds

DIVISION OF PHARMACEUTICAL CHEMISTRY
FACULTY OF PHARMACY
UNIVERSITY OF HELSINKI

Division of Pharmaceutical Chemistry
Faculty of Pharmacy
University of Helsinki
Finland

DIRECT OPEN AIR SURFACE SAMPLING/IONIZATION MASS SPECTROMETRY METHODS IN THE STUDY OF NEUTRAL AND NONPOLAR COMPOUNDS

Anu Vaikkinen

ACADEMIC DISSERTATION

To be presented, with the permission of the Faculty of Pharmacy of the University of Helsinki, for public examination in lecture hall 6, Viikki B-building (Latokartanonkaari 7), on October the 18th, 2013, at 12 o'clock noon.

Helsinki 2013

Supervisors
Docent Tiina J. Kauppila
Division of Pharmaceutical Chemistry
Faculty of Pharmacy
University of Helsinki
Finland

Professor Risto Kostiainen
Division of Pharmaceutical Chemistry
Faculty of Pharmacy
University of Helsinki
Finland

Reviewers
Professor Graham Cooks
Department of Chemistry
Purdue University
USA

Professor Facundo M. Fernández
School of Chemistry and Biochemistry
Georgia Institute of Technology
USA

Opponent
Professor Luke Hanley
Department of Chemistry
University of Illinois at Chicago
USA

ISBN 978-952-10-9270-1 (pbk.)
ISBN 978-952-10-9271-8 (PDF)
ISSN 1799-7372
Helsinki University Print
Helsinki 2013

ABSTRACT

Direct open air surface sampling/ionization mass spectrometry offers a means to the rapid, sensitive, and reliable analysis of samples in their native states. The methods have been applied for screening, fingerprinting, and mass spectrometry imaging (MSI) in areas of quality control, biological research, forensic investigation, and homeland and public security. The sampling can be achieved by thermal desorption, liquid or gas jet surface impact, laser ablation, liquid extraction, or mechanical pick-up, while the ionization typically occurs by electrospray, chemical ionization, or photoionization. The sampling mechanism of the used method determines the smallest possible surface area and volume that can be analyzed. Small sampling areas (or volumes) are required for study of biologically relevant cell populations, single cells and cell organelles. The ionization mechanism determines which compounds will be detected. Electrospray-based techniques are best suited for polar and ionic analytes, while the chemical and photoionization-based methods facilitate the study of neutral and nonpolar compounds. Photoionization is an excellent tool even for completely nonpolar compounds, such as polyaromatic hydrocarbons (PAHs), since it allows the ionization of low proton affinity analytes by charge exchange. The aim of this work was to develop and apply direct open air surface sampling/ionization mass spectrometry methods in the study of neutral and nonpolar compounds, with emphasis on photoionization-based techniques.

First, two krypton discharge photoionization lamps typically used in atmospheric pressure photoionization were compared in micro atmospheric pressure photoionization and desorption atmospheric pressure photoionization mass spectrometry (DAPPI-MS) studies. The radio frequency (rf) alternating current lamp emitted 5 times the number of photons of the direct current (dc) lamp. The reason is the broader light beam of the rf lamp. The rf lamp was also shown to have even over an order of magnitude higher ionization efficiency than the dc lamp in both positive and negative ion modes. The difference in ionization efficiency was greatest with solvents of low ionization energy.

Direct open air surface sampling/ionization mass spectrometry methods are mainly intended for analyses without prior sample preparation, but matrix effects are severe for complex biological samples. As a remedy, a polydimethylsiloxane (PDMS) extraction phase was developed and optimized for DAPPI-MS analyses of aqueous samples. Effort was put into oligomer removal to avoid spectral disturbance from ions originating in PDMS. With six model analytes, including two PAHs and a steroid, the linearity of the developed method was confirmed (1.5 decades, r^2 0.9815-0.9991), and limits of detection (LODs) were in the 10-90 nM range. The analysis of spiked wastewater and urine samples demonstrated that the method did, indeed, reduce matrix effects and could effectively be used for the MS screening of nonpolar compounds in real samples.

The direct open air surface sampling/ionization mass spectrometry methods best suited for neutral and nonpolar analytes mostly rely on sampling methods that

do not enable analyses at sub-millimeter range, and thus they are not optimal for MSI. A novel, laser ablation atmospheric pressure photoionization (LAAPPI) ion source was developed to enable such analyses. In the LAAPPI source, the sample is ablated with a mid-infrared (mid-IR) laser at 2.94 μm. The laser excites the OH bonds of endogenous water contained by biological tissues, causing a miniature explosion and ejection of the sample material from quasi-circular areas of approx. 300 μm diameter. The ejected projectiles are exposed to a hot solvent jet for vaporization and are subsequently ionized by a krypton discharge photoionization lamp. The LAAPPI method was capable of semi-quantitative performance and suited for the analysis of neutral and nonpolar compounds directly from plant (*Citrus aurantium* leaves) and animal (rat brain) tissues. Subsequent work also demonstrated the suitability of LAAPPI for MSI. In this case, phytochemicals of sage (*Salvia officinalis*) leaves were studied. Leaf structural elements could be distinguished and, with the aid of correlation analysis, LAAPPI was confirmed to be a useful tool for the study of leaf metabolism.

The final part of the research involved the modification of a laser ablation electrospray ionization (LAESI) source with a heated gas jet to enable the simultaneous study of polar and nonpolar compounds. In conventional LAESI, the sample is ablated by a mid-IR laser and the ablated material is ionized by electrospray. In the modified setup, the sample projectiles were sprayed with an electrospray plume and a heated nitrogen jet. Heat-assisted LAESI (HA-LAESI) was tested for analytes of different polarities and sizes, and it was found to protonate compounds ranging from selected PAHs to large proteins with more or less equal efficiency. As compared with LAAPPI and LAESI, the HA-LAESI method ionized a wider range of analytes. It was semi-quantitative, and LODs were in the low picomole range. Avocado (*Persea americana*) fruit and mouse brain tissue were successfully fingerprinted, confirming that neutral and nonpolar analytes can be detected in biological matrices. MSI was demonstrated by the study of pigments from pansy (*Viola*) petals.

In conclusion, the work presented in this thesis advances the study of neutral and nonpolar compounds through developments in direct open air surface sampling/ionization mass spectrometry. Like other direct open air surface sampling/ionization mass spectrometry methods, however, the described methods are still in their infantry. Additional work is required to establish them as reliable competitors of more traditional techniques.

PREFACE

The work described in this thesis was carried out in the Division of Pharmaceutical Chemistry of the Faculty of Pharmacy, University of Helsinki, during 2009-2013. Some of the data were collected at the Department of Chemistry, George Washington University, in 2011 and 2012. Funding was provided by the Academy of Finland and the CHEMSEM Graduate School.

First and foremost, I would like to thank my supervisors Docent Tiina J. Kauppila and Professor Risto Kostiainen, for giving me the opportunity to work in the Division of Pharmaceutical Chemistry. Their ideas and guidance have made my thesis a reality.

I am also grateful to Professor Akos Vertes from the George Washington University for welcoming me to his laboratory. Although not my official supervisor, his guidance and feedback have been invaluable.

I would like to thank Dr Bindesh Shrestha from George Washington University, who taught me how to use the IR laser. Warm thanks go as well to Dr Markus Haapala, who has a thorough knowledge of just about everything related to instrumentation and was always ready to share. My other co-authors are warmly thanked for their contributions: Tapio Kotiaho for informative discussion, Hendrik Kersten and Thorsten Benter for the UV emission measurements, Juha Koivisto for being by my side all these years and serving as a code monkey at just the right moment, and Javad Nazarian for the gift of mouse brain.

Professors Graham Cooks and Facundo Fernández are warmly thanked for their insightful comments on the thesis.

Further thanks are extended to all those involved in the development of the heated nebulizer microchips, which have played such an essential role throughout this work.

The inspiration provided by the Inkun kahvisalonki and indeed by all those working in the Division of Pharmaceutical Chemistry and the Vertes lab is enthusastically acknowledged. You made my day, every day. Last, and certainly not least, loving thanks go to my family for their unfailing support.

CONTENTS

LIST OF ORIGINAL PUBLICATIONS

This thesis is based on the following publications:

I Anu Vaikkinen, Markus Haapala, Hendrik Kersten, Thorsten Benter, Risto Kostiainen, and Tiina J. Kauppila, Comparison of direct and alternating current vacuum ultraviolet lamps in atmospheric pressure photoionization, Analytical Chemistry, 2012, 84, 1408−1415

II Anu Vaikkinen, Tapio Kotiaho, Risto Kostiainen, and Tiina J. Kauppila, Desorption atmospheric pressure photoionization with polydimethylsiloxane as extraction phase and sample plate material, Analytica Chimica Acta, 2010, 682, 1–8

III Anu Vaikkinen, Bindesh Shrestha, Tiina J. Kauppila, Akos Vertes, and Risto Kostiainen, Infrared Laser Ablation Atmospheric Pressure Photoionization Mass Spectrometry, Analytical Chemistry, 2012, 84, 1630−1636

IV Anu Vaikkinen, Bindesh Shrestha, Juha Koivisto, Risto Kostiainen, Akos Vertes, and Tiina J. Kauppila, Laser Ablation Atmospheric Pressure Photoionization Mass Spectrometry Imaging of Phytochemicals from Sage Leaves (submitted)

V Anu Vaikkinen, Bindesh Shrestha, Javad Nazarian, Risto Kostiainen, Akos Vertes, and Tiina J. Kauppila, Simultaneous Detection of Nonpolar and Polar Compounds by Heat-Assisted Laser Ablation Electrospray Ionization Mass Spectrometry, Analytical Chemistry, 2013, 85, 177−184

The publications are referred to in the text by their roman numerals.

Author's contribution to the publications included in this thesis:

I All mass spectrometry data was acquired by the author, while the UV emission measurements were carried out by Hendrik Kersten. The manuscript was written by the author with contributions from others.

II The experimental work was carried out by the author. The manuscript was written by the author with contributions from others.

III The experimental work was carried out by the author and Bindesh Shrestha. The manuscript was written by the author with contributions from others.

IV The mass spectrometry data was acquired by the author with contributions from Bindesh Shrestha. The algorithm for data processing was written by Juha Koivisto with contributions from the author. The manuscript was written by the author with contributions from others.

V The experimental work was carried out by the author with contributions from Bindesh Shrestha. The manuscript was written by the author with contributions from others.

ABBREVIATIONS AND SYMBOLS

APCI	atmospheric pressure chemical ionization
API	atmospheric pressure ionization
APPI	atmospheric pressure photoionization
ASAP	atmospheric pressure solids analysis probe
CI	chemical ionization
DAPCI	desorption atmospheric pressure chemical ionization
DAPPI	desorption atmospheric pressure photoionization
DART	direct analysis in real time
dc	direct current
DEMI	desorption electrospray/metastable-induced ionization
DESI	desorption electrospray ionization
DHEA	dehydroepiandrosterone
DICE	desorption ionization by charge exchange
EI	electron impact
ELDI	electrospray-assisted laser desorption/ionization
ES	electrospray
ESI	electrospray ionization
GC	gas chromatograph/gas chromatography
HA-LAESI	heat-assisted laser ablation electrospray ionization
IE	ionization energy
IR	infrared
IR-LAMICI	infrared laser ablation metastable-induced chemical ionization
LAAPPI	laser ablation atmospheric pressure photoionization
LAESI	laser ablation electrospray ionization
LA-FAPA	UV laser ablation flowing atmospheric-pressure afterglow
LC	liquid chromatography
LDI	laser desorption ionization
LOD	limit of detection
m/z	mass-to-charge ratio
MALDESI	matrix-assisted laser desorption electrospray ionization
MALDI	matrix-assisted laser desorption/ionization
MS	mass spectrometry/mass spectrometer
MSI	mass spectrometry imaging
OPO	optical parametric oscillator
PA	proton affinity
PAH	polyaromatic hydrocarbon
PDMS	polydimethylsiloxane
PMMA	poly(methyl methacrylate)
rf	radio frequency
S/N	signal-to-noise ratio
SESI	secondary electrospray ionization

SIMS	secondary ion mass spectrometry
TG	triglyceride
TLC	thin layer chromatography
TMCL	1,1′,2,2′-tetramyristoyl cardiolipin
UV	ultraviolet
VUV	vacuum ultraviolet
μAPPI	micro atmospheric pressure photoionization

1 INTRODUCTION

Mass spectrometry (MS) is a versatile analytical technique with high sensitivity and selectivity. A mass spectrometric analysis consists of three steps: generation of analyte gas-phase ions in an ion source, separation of the ions in an analyzer according to their mass-to-charge ratios (m/z), and detection of the separated ions. The selection of the ion source is critical in determining the kinds of compounds that will be detected, as well as the sample types that can be analyzed.

Initially, MS ion sources were operated at low pressure, and electron impact (EI) was a typical ion source. The EI source was interfaced with a gas chromatograph (GC) in the 1950s,[1] and despite the extensive analyte fragmentation in EI, GC-EI-MS remains a popular technique. In 1966, Munson and Field[2] introduced a chemical ionization ion source (CI), which exploited reactions observed previously by Tal'rose.[3] CI facilitates molecular mass determinations by producing more stable ions characteristic of the molecular mass of the analyte. However, CI, and alternative techniques such as secondary ion MS (SIMS), field desorption, and laser desorption ionization were not suitable for the analysis of large nonvolatile or thermally unstable biomolecules like polypeptides and proteins. Furthermore, liquid chromatography (LC) could not be efficiently combined with MS because the capacity of the vacuum pumps was too low to allow evacuation of the whole volume of vaporized LC eluent needed to achieve the pressure required by the analyzer. In 1973, Horning *et al.*[4] demonstrated an atmospheric pressure chemical ionization (APCI) source for combining LC and MS. The introduction of various solvent splitting and molecular separator techniques and gradual evaporation in a moving belt interface improved the interfacing and provided advances in small molecule bioanalysis, but the detection of large and thermolabile molecules was still not feasible.

Two major breakthroughs were achieved in the 1980s. Tanaka *et al.*[5] generated ions of up to m/z 100 000 by a method similar to the matrix-assisted laser desorption/ionization (MALDI) developed by Karas and Hillenkampf,[6, 7] while Fenn and co-workers showed that electrospray ionization (ESI)[8] at atmospheric pressure can be combined with mass spectrometry[9] to enable the study of large biomolecules.[10] MALDI is now widely used in proteomics and other bioapplications, while ESI accelerated the development of atmospheric pressure ionization (API) source interfaces and soon became the most widely applied LC-MS ionization method for all polar molecules, big and small. APCI increased in popularity, thanks to the development of interfaces, and because it is more effective than ESI for certain lower polarity analytes. The polarity range of LC-API sources was further extended in 2000 when two independent groups[11, 12] introduced atmospheric pressure photoionization (APPI) for the ionization of completely nonpolar compounds.

During the last decade, the growing need for faster analyses and improved reliability has led to exploration of MS as a detector for rapid, direct study of objects

of interest. Direct MS of solids had been applied earlier when samples were introduced with a solids analysis probe or ionized by a desorption ionization technique such as field desorption, fast atom bombardment, plasma desorption, SIMS, or MALDI. However, the development of the API interfaces opened up new avenues: for when ionization occurs outside the mass spectrometer, sample switching is quick and there are fewer restrictions on sample size or shape. The ambient sampling environment also helps to reach *in vivo*-like conditions in bionalyses, in contrast to vacuum, which may destroy the sample integrity. Matrix-assisted ionization of solids in atmospheric pressure has been demonstrated with use of direct insertion probes in APCI[13] and more popularly in the atmospheric pressure version of MALDI.[14] Direct matrix-free surface analyses were demonstrated in the early 2000s when Van Berkel *et al.*[15] used extractive sampling probes to study analytes separated on thin layer chromatography (TLC) plates, and Coon *et al.*[16] used laser desorption APCI for the analysis of peptides from electrophoresis gels.

Direct open air surface sampling/ionization MS analysis gained increasing attention after 2004, when desorption electrospray ionization (DESI) was introduced.[17] A similar method, direct analysis in real time (DART), was developed about the same time and published a year later.[18] The introduction of DESI and DART encouraged the development of many other techniques aimed at the same task:[19-21] rapid analysis of the surfaces of native objects of various sizes and shapes with minimal need for sample preparation or pre-separation. The MS literature refers to these techniques as direct open air surface sampling/ionization mass spectrometry,[20] atmospheric pressure surface sampling/ionization techniques,[21] or ambient MS.[19] The latter includes also other than surface sampling techniques.

The work described in this thesis was aimed at developing and applying direct open air surface sampling/ionization mass spectrometry methods for the analysis of neutral and nonpolar compounds, which usually are inefficiently ionized by the popular electrospray-based techniques. The study of these types of compounds is typically driven by their carcinogenic or environmentally harmful properties (e.g., PAHs) or biological roles in health and sickness (e.g., triglycerides, cholesterol). Two photoionization lamps were studied in DAPPI and μAPPI, two novel ion sources (laser ablation atmospheric pressure photoionization, LAAPPI, and heat-assisted laser ablation electrospray ionization, HA-LAESI) and a sample preparation method for DAPPI were developed, and the utility of the newly developed laser ablation atmospheric pressure photoionization source in mass spectrometry imaging (MSI) was demonstrated.

1.1 DIRECT OPEN AIR SURFACE SAMPLING/IONIZATION MASS SPECTROMETRY METHODS

Direct open air surface sampling/ionization mass spectrometry covers methods that ionize compounds on sample surfaces in the ambient laboratory or field environment with detection by MS. Since the introduction of DESI[17] and DART,[18] direct open air surface sampling/ionization mass spectrometry has developed into a complete family of methods. Table 1 gives a representative but not complete list of the existing methods. More comprehensive lists can be found in references 20 and 21. Selected methods are introduced below.

1.1.1 DESORPTION ELECTROSPRAY IONIZATION AND DESORPTION IONIZATION BY CHARGE EXCHANGE

Desorption electrospray ionization[17] (DESI) uses a simple experimental set-up where a spray of charged solvent droplets is aimed at the sample to desorb compounds from its surface. The DESI spray is produced by creating a potential difference of ~1-8 kV between a hypodermic needle (the electrospray (ES) emitter), and the mass spectrometer inlet and pumping solvent through the needle. The spray is produced with the aid of nebulizer gas, typically nitrogen. The desorption and ionization occur in a single step, likely by the droplet pick-up mechanism.[22-24] When the spray droplets collide with the sample, they spread out to form a thin liquid film on the surface. Secondary droplets, which hit the film and/or are released from its edges when expanding, remove sample molecules from the surface. After the desorption, the ionization occurs as in electrospray ionization,[22] via ion evaporation[25] and/or by charged residue[8] mechanism.

Because of the ESI-like ionization mechanism, under typical operating conditions DESI is best suited for polar and ionic compounds. The ionization efficiency for neutral and nonpolar compounds is lower,[22, 26] but can be improved by choosing a small spray impact angle and large spray-to-sample surface distance,[22] or by using nonpolar spray solvents, which enhance their solubility in the spray.[26, 27] An alternative method of producing ions of neutral and nonpolar compounds (e.g., steroids) by DESI is to have them react with species added to the spray solvent.[28, 29] While reactive DESI is suited for targeted analysis, its selectivity and specificity make it less useful in the study of unknown analytes and multicomponent mixtures.

Desorption ionization by charge exchange (DICE) is closely related to DESI and employs a similar setup.[30] In DICE, toluene is used as the spray solvent and the formation of the spray is assisted thermally (~350 °C). Electrochemical reactions in the emitter form toluene radical cations that react with the sample molecules by charge-exchange reactions. This means that DICE is able to ionize neutral and nonpolar compounds, which have low proton affinities (PAs) and low protonation efficiency (e.g., by DESI), but have ionization energies (IEs) below that of toluene.

Table 1. *Representative currently available direct open air surface sampling/ionization techniques (adopted from Van Berkel et al.).*[21] *SSI = sonic spray ionization, * requires external matrix*

Name of technique	Acronym	Sampling by	Ionization by	ref
Thermal desorption/ionization				
Atmospheric pressure thermal desorption ionization	APTDI	Thermal desorption	liberation of organic salt from surface	31
Thermal desorption atmospheric pressure chemical ionization	TD/APCI	Thermal desorption	APCI, corona discharge	32
Desorption atmospheric pressure chemical ionization	DAPCI	Thermal desorption	APCI, corona discharge	33
Direct analysis in real time	DART	Gas impact/thermal desorption	APCI, glow discharge	18
Atmospheric pressure solids analysis probe	ASAP	Thermal desorption	APCI, corona discharge	34
Desorption atmospheric pressure photoionization	DAPPI	Thermal desorption	photoionization	35
Laser ablation/post-ionization				
Laser desorption atmospheric pressure chemical ionization	LD-APCI	IR laser ablation	APCI, corona discharge	16
Infrared laser ablation metastable-induced chemical ionization	IR-LAMICI	IR laser ablation	APCI, glow discharge	36
Electrospray-assisted laser desorption/ionization	ELDI	UV laser ablation	ESI	37
Laser ablation electrospray ionization	LAESI	IR laser ablation	ESI	38
Matrix-assisted laser desorption electrospray ionization	MALDESI	UV laser ablation*	ESI	39
UV laser ablation flowing atmospheric-pressure afterglow	LA-FAPA	UV laser ablation	APCI, flowing afterglow	40
Laser-induced acoustic desorption/electrospray ionization	LIAD/ESI	Laser induced acoustic desorption	ESI	41
Liquid and/or gas jet desorption/ionization				
Plasma-assisted desorption/ionization	PADI	Plasma jet surface impact	APCI, cold plasma	42
Desorption electrospray ionization	DESI	Charged droplet surface impact	ESI	17
Easy ambient sonic spray ionization	EASI	Neutral droplet/gas jet surface impact	SSI	43
Desorption ionization by charge exchange	DICE	Charged droplet/gas stream surface impact	charge exchange	30
Liquid extraction or mechanical sampling/ionization				
Liquid microjunction surface sampling probe	LMJ-SSP	Liquid extraction	ESI	15
Probe electrospray ionization	PESI	Mechanical pick-up	ESI	44
Multimode sources				
Desorption electrospray/metastable-induced ionization	DEMI	Charged droplet surface impact	ESI and APCI	45
Desorption ionization by charge exchange (DICE) and desorption electrospray ionization (DESI) combined	DICE + DESI	Charged droplet surface impact	ESI and charge exchange	46

1.1.2 DIRECT ANALYSIS IN REAL TIME AND DESORPTION ATMOSPHERIC PRESSURE CHEMICAL IONIZATION

In direct analysis in real time (DART),[18] a stream of excited-state species, typically helium metastables, desorbs and ionizes molecules from the sample surface. The metastables are created by exposing neutral gas to a glow discharge[18, 47] and removing formed ions and electrons from the stream. The metastable stream can be directed to the mass spectrometer inlet and the sample is then dipped into the stream. Alternatively, the reaction gas can be directed to the sample surface in a geometry similar to that applied in DESI. The gas stream can be heated, and the desorption is most likely thermal, as increase of the heating temperature generally increases the analyte signals.[48-53] Efficiency of the ion transmission depends on complex interactions of fluid dynamics, heat transfer, and electrostatic phenomena within the sampling region.[54] Ionization of the analyte is thought to occur by direct Penning ionization (Reaction 1, Scheme 1),[18] or more likely by a reaction cascade where the excited gas species (typically He excited to the 2^3S electronic state with 19.8 eV energy) first reacts with ambient water (clusters) via Reaction 2 (Scheme 1),[18] or Reactions 1 and 3 (Scheme 1),[55, 56] and then the water (cluster) ions protonate the analyte molecules (M, Reaction 4, Scheme 1). Under special conditions, where the humidity of the source is kept low, ambient oxygen can play a role in the ionization process.[47] It has been suggested that oxygen is ionized by Penning ionization (Reaction 1, Scheme 1, N = O_2) and further reacts with the analytes by charge exchange (Reaction 5, Scheme 1),[47] enabling the ionization of compounds with low PA and low IE. Reactions with ambient ammonium ions are also possible (Reaction 6, Scheme 1),[18, 47] and the ionization process can be manipulated by adding other suitable reagents to the ionization region.[47, 55]

Scheme 1. *Ionization reactions occurring in the DART source [18, 47] G = reaction gas, G* = gas metastable, N = ambient/additive/matrix neutral, M = analyte molecule*

Reaction	**#**
$G^* + N \rightarrow N^{+\cdot} + G + e^-$	1
$G^* + (H_2O)_n \rightarrow [(H_2O)_{n-1}H]^+ + OH^- + G$	2
$N^{+\cdot} + N_n \rightarrow [N\text{-}H]^\cdot + [N_n+H]^+$	3
$[N_n+H]^+ + M \rightarrow MH^+ + N_n$	4
$N^{+\cdot} + M \rightarrow N + M^{+\cdot}$	5
$NH_4^+ + M \rightarrow [M+NH_4]^+$	6

In desorption atmospheric pressure chemical ionization (DAPCI),[33] molecules are desorbed from a sample surface by heated solvent or gas stream, and the desorbed neutrals are ionized by corona discharge. The discharge voltage is typically 3-6 kV, and water/methanol, toluene, or methanol, for example, can be used as the spray solvent. The discharge is believed to ionize the air and/or solvent molecules as in APCI.[33, 57] Thus the ionization reactions are similar to Reactions 4 and 5 in DART (Scheme 1), depending on the solvents employed. DAPCI provides better sensitivity than DESI for neutral, low-polarity hydrocortisone,[58] and a comparison of DART, DESI, and DAPCI showed DAPCI to provide best ionization efficiency for various compounds of low to moderate polarity.[59]

1.1.3 DESORPTION ATMOSPHERIC PRESSURE PHOTOIONIZATION

Desorption atmospheric pressure photoionization[35] (DAPPI, Figure 1) uses a heated solvent jet to desorb molecules from sample surfaces. The desorption is thought to be mainly a thermal process[35, 60] that can be enhanced by increasing the temperature of the spray solvent jet[35] or by choosing an appropriate low thermal conductivity sampling surface,[60] since low conductivity promotes local heating and thus analyte evaporation. The ionization is initiated by a krypton discharge vacuum ultraviolet photoionization lamp that emits 10.0 and 10.6 eV photons and is aimed at the sampling surface.

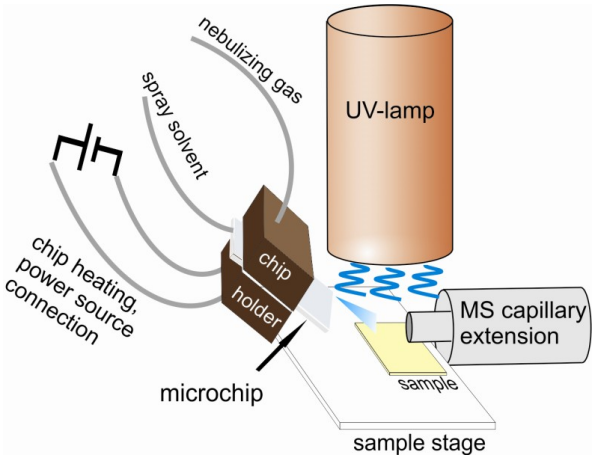

Figure 1 Schematic representation of the DAPPI ion source.

The ionization mechanism of DAPPI is considered to be similar to that in APPI.[35, 60] The lamp photons can release an electron from the analyte if the IE of the analyte is lower than the energy of the photons (Reaction 1, Scheme 2).[11, 12, 61] However, as shown in APPI studies, direct analyte ionization is often inefficient,[12, 61] and ionization more likely occurs via gas-phase reactions with solvent ions formed in Reaction 2 (Scheme 2). For efficient ionization to occur, consequently, the IE of the DAPPI spray solvent must be below the energy of the photons (10.0 and 10.6 eV). Toluene (IE 8.8 eV),[62] anisole (IE 8.2 eV),[62] acetone (IE 9.7 eV),[62] hexane (IE 10.1 eV),[62] 2-propanol (IE 10.2 eV),[62] and mixtures of methanol with toluene and acetone are suitable DAPPI solvents.[35, 60] Pure methanol (IE 10.8 eV)[62] did not produce analyte ion signals in early experiments.[35]

If the IE of the analyte is below the recombination energy (≈IE) of the solvent radical cation, the analyte can be ionized by charge exchange with the solvent ion (Reaction 3, Scheme 2).[12, 61] Charge exchange is a prominent reaction in the DAPPI analysis of PAHs, for example.[63] If the analyte has high proton affinity, above that of the solvent radical cation, ionization can occur by proton transfer (Reaction 4, Scheme 2).[12, 61, 64] An alternative mechanism for MH^+ ion formation in APPI has also

been suggested: an analyte radical cation can abstract a hydrogen atom from a protic solvent, such as methanol (Reaction 5, Scheme 2).[11, 65]

Scheme 2. *Ionization reactions occurring in DAPPI and APPI. hν = photon energy, S = solvent, M = analyte, D_H = hydrogen bond energy*

Reaction	Notes	#
$h\nu + M \rightarrow M^{+\cdot} + e^-$	$IE(M) < h\nu$	1
$h\nu + S \rightarrow S^{+\cdot} + e^-$	$IE(S) < h\nu$	2
$S^{+\cdot} + M \rightarrow S + M^{+\cdot}$	$IE(M) < RE(S) \approx IE(S)$	3
$S^{+\cdot} + M \rightarrow [S\text{-}H]^{\cdot} + [M+H]^+$	$PA(M) > PA([S\text{-}H]^{\cdot})$	4
$M^{+\cdot} + S \rightarrow [M+H]^+ + [S\text{-}H]^{\cdot}$	$\Delta H = IE(H) - IE(M) - PA(M) + D_H(S)$	5
$[S+H]^+ + M \rightarrow [M+H]^+ + S$	$PA(M) > PA(S)$	6
$e^- + M \rightarrow M^{-\cdot}$	$EA(M) > 0$	7
$O_2^{-\cdot} + M \rightarrow M^{-\cdot} + O_2$	$EA(M) > EA(O_2)$	8
$O_2^{-\cdot} + M \rightarrow [M\text{-}H]^- + HO_2^{\cdot}$	$\Delta G_{acid}(M) < \Delta G_{acid}(HO_2^{\cdot})$	9

Solvent radical cations are not observed when high PA spray solvents such as acetone are used.[60] A likely explanation of this is rapid self-protonation (Reaction 4 or 5, Scheme 2, where M=S).[64] The solvent SH^+ ions can protonate the analytes via Reaction 6 (Scheme 2).[60, 61, 66] More complicated ionization processes can be expected with solvent mixtures, as has been shown in APPI,[61, 64] and even small amounts of suitable solvent or impurity can affect the ionization process.[61, 67] As example, with mixtures of methanol and toluene, methanol (clusters) can be ionized by proton transfer with toluene (Reaction 4, Scheme 2) and react with the analytes via proton transfer (Reaction 6, Scheme 2). Other reactions can occur as well: DAPPI has been shown to produce analyte $[M\text{-}H]^+$ and $[M+NH_4]^+$ ions, along with diverse fragmentation products.[68]

Although fewer studies have been made on negative ion mode DAPPI,[60] reactions similar to those in APPI are likely to occur. In APPI, the electrons produced in Reaction 2 (Scheme 2)[61, 69] or released from the metal surfaces of the ion source[70] are rapidly thermalized in the ion source and can be captured by the analytes (Reaction 7, Scheme 2).[69, 71, 71] Since oxygen has high electron affinity, $O_2^{-\cdot}$ ions are formed in the source owing to the presence of air.[61, 69, 72] Oxygen radical anions can ionize the analytes via charge exchange and proton transfer (Reactions 8 and 9 in Scheme 2, respectively).[60, 61, 69, 72] Additional negative ionization APPI reactions include fragmentation,[61, 69] substitution,[69] oxidation,[60, 61] and anion attachment.[72]

In conclusion, the charge-exchange reactions of DAPPI provide a feasible ionization route for low IE compounds that have low PA and hence do not easily protonate (in DESI, DAPCI, or DART, for example). A few comparisons of DAPPI and DESI have been made[68, 73] and, as expected, DESI has shown lower ionization efficiency than DAPPI towards fat soluble vitamins and cholesterol.[68] More work is needed to elaborate the differences between the performances of DAPPI and DART. In view of the ionization mechanism, the development of photoionization-based methods for direct open air surface desorption/ionization MS would seem a feasible strategy to pursue in the study of neutral and nonpolar compounds.

1.1.4 LASER ABLATION POST-IONIZATION

In laser ablation post-ionization techniques, sampling and ionization occur in two separate steps. First, the target is sampled by laser ablation and then the ablated neutrals are ionized. Two main types of lasers have been applied for the ablation: ultraviolet (UV) lasers, operating, for example, at 266 nm (Nd:YAG)[40] and 337 nm (N_2),[37, 39] and IR lasers, operating, for example, at 2.94 μm (Nd:YAG/OPO)[36, 38] and 10.6 μm (CO_2).[16] Similar lasers have been utilized in vacuum and AP-MALDI[74] as well as in laser desorption ionization (LDI). It is thought that the laser irradiation is absorbed by the target, leading to rapid heating, phase explosion, and the ejection of sample projectiles, which can be in gas, liquid, or solid phase. In the case of IR lasers, the wavelength is chosen on the basis of the vibrational excitation of the molecules in the sample, 2.94 μm for the OH bond of water, for example.[38, 75] Thus endogenous water of biological tissues absorbs the laser photons and can act as a native ablation-enhancing matrix.[76] With UV lasers, the absorption occurs by electronic excitation. Where analyte molecules are non-absorbing in the UV range, an external matrix can be applied to enhance sample ablation in a manner similar to MALDI (as in matrix-assisted laser desorption electrospray ionization (MALDESI), for example).[39] A matrix-free approach has also proven feasible, as in electrospray-assisted laser desorption/ionization (ELDI).[37] Although a matrix renders the ablation more efficient,[39] the matrix-free approach provides minimal need for sample preparation and the native distributions of compounds on the sample are not disturbed by application of the matrix.[77] The matrix-free ablation should be especially efficient for compounds containing conjugated double bonds (i.e., delocalized π-electrons), as has been demonstrated in LDI.[78, 79]

After the ablation, the ejected plume is ionized and guided to the mass spectrometer. The ionization is achieved by orthogonal electrospray in laser ablation electrospray ionization (LAESI),[38] ELDI,[37] and MALDESI;[39] by chemical ionization-type reactions initiated by corona discharge in LD-APCI;[16] by DART-type metastables in infrared laser ablation metastable-induced chemical ionization (IR-LAMICI);[36] and by flowing afterglow plasma in UV laser ablation flowing atmospheric-pressure afterglow (LA-FAPA).[40] When electrospray is used for the ionization, the neutral ablated projectiles are picked up by the electrospray droplets directed at the MS inlet and ionized in a typical ESI process[38, 39] according to ion evaporation[25] and/or charged residue[8] models. In IR-LAMICI, the flow of the metastable stream is thought to push the neutrals to the MS, simultaneously ionizing the analytes.[36] In LA-FAPA, the ionizing plume directed at the MS is believed to desorb the analytes from neutral solid projectiles and ionize them before the MS analysis.[40]

1.1.5 MULTIMODE METHODS

In addition to the ion sources applying a single ionization method, two multimode methods have been introduced aiming at more universal ionization capabilities.[45, 46] Desorption electrospray/metastable-induced ionization (DEMI) desorbs the analytes with a charged solvent spray, and ionization occurs by electrospray and chemical ionization (DART)-type reactions.[45] The second method mixes polar and nonpolar solvents in a DESI-type setup, and ionization occurs much as in DESI and DICE.[46] Both methods ionize polar and nonpolar compounds simultaneously, unlike the single ionization methods. In addition, photoionization has recently been combined with DART.[80] Compared with the typical DART source, the introduction of the lamp enhanced the ionization efficiency of cortisol and anthracene but also of more polar compounds, such as verapamil. Comparisons with DAPPI have not yet been made and it is not known whether the performance is superior or similar to DAPPI.

1.2 APPLICATIONS OF DIRECT OPEN AIR SURFACE SAMPLING/IONIZATION MASS SPECTROMETRY

Two important uses of direct open air surface sampling/ionization mass spectrometry are screening and fingerprinting. Typical samples and analytes are pharmaceuticals,[59, 81, 82] confiscated items,[83] residues of hazardous chemicals,[32, 84] synthesis products,[85] oils,[86] polymers,[87] food products,[17, 63, 88] and biological materials of clinical, environmental and research interest.[49, 89-93] Quality control, metabolite profiling, homeland and public security, and forensics are typical areas of application. Comprehensive reviews of the applications are presented in references 94 and 95, and Table 2 lists examples of applications targeted at the analysis of neutral and nonpolar compounds without the need for traditional sample preparation. DART, DAPPI, and reactive DESI are the clear methods of choice for the detection of the most nonpolar analytes (PAHs, hydrocarbons, steroids) in complex multicomponent matrices. Triglycerides have been analyzed with DESI and EASI because they readily form adduct ions with these methods. Although comprehensive comparisons of methods have not been made, it bears notice that reactive DESI is only suited for targeted analysis because the reagents are functional-group specific. Further, a successful analysis of soil pellets with DAPPI[63] suggested that DAPPI is especially sensitive toward nonpolar compounds, as the analyte concentrations were only 10 μg/g.

Table 2. *Applications of direct open air surface sampling/ionization mass spectrometry methods in the analysis of neutral and nonpolar compounds. REIMS = rapid evaporative ionization MS, LTP probe = low temperature plasma probe, HPTLC = high performance TLC, LIAD-CI = laser induced acoustic desorption chemical ionization*

Method	Sample	Studied analytes	Notes	Ref
LIAD-CI	base oil	saturated hydrocarbons	detected mainly as $[M-H]^+$	96
reactive DESI	petroleum distillates	C_{21}-C_{30} saturated hydrocarbons	oxidation + betaine aldehyde reagent	97
DART	flies *in vivo*	C_{18}-C_{29} hydrocarbons	detected as MH^+ ions	92
DAPPI	spiked soil pellets	PAHs	detected as $M^{+\cdot}$ ions	63
DART	synthesis products	large, insoluble PAHs	detected as $M^{+\cdot}$ and MH^+ ions	56
DAPPI and DESI	α-tocopherol capsules	α-tocopherol	DAPPI shows better ionization efficiency, DAPPI: $M^{+\cdot}$, DESI: MH^+	68
DART	leaves and stems of eucalyptys	terpenes and terpenoids	detected as MH^+ ions	49
ASAP	spinach leaves	carotenoids		34
reactive DESI	tissue sections	cholesterol	betaine aldehyde as the reagent	98
DAPPI	brain tissue	cholesterol	detected as $[MH-H_2O]^+$	99
DAPPI and DESI	butter	cholesterol	detected as $[MH-H_2O]^+$, not detected with DESI	68
reactive DESI	urine	anabolic steroids	hydroxylamine as the reagent	29
DESI	spiked urine	steroids	detected as Na^+ adducts	100
DESI	(pro)hormone preparations and supplements	steroids		101
DAPPI	ampules	steroids and steroid esters		102
DESI	multivitamin tablets	vitamin D2, lycopene		81
ASAP	fungal cells	sterols: lanosterol, ergosterol		103
HPTLC-EASI	soybean oil	triglycerides	detected as Na^+ adducts	104
EASI	mouse liver	triglycerides	detected as Na^+ and K^+ adducts	105
EASI	vegetable oils	triglycerides	detected as Na^+ adducts	86, 106
DART	olive oil	triglycerides	detected as MH^+ (no dopant) or NH_4^+ adducts (with NH_3 dopant)	50
DESI	edible oils	triglycerides	detected mainly as NH_4^+, Na^+, and K^+ adducts	107
REIMS	mammal tissues	triglycerides	detected as NH_4^+ adducts	90
DESI	rat spinal cord	diglycerides	detected as $[M-H]^-$	108
DART	grapefruit	bergamottin	detected as MH^+ ion	109
LTP probe	petroleum crude oil	low to moderate polarity compounds		110
DART	wheat, maize	mycotoxins		111
DART	plastics, plastisols, toys	neutral plasticizers		112-114
DART	hair, towels	fragrances		115

Matrix and suppression effects frequently interfere with direct open air surface sampling/ionization MS analysis,[53, 55, 73, 116, 117] especially in the case of complex biological samples. Quantitative performance has been achieved without sample preparation in only a few studies.[51, 53, 82, 84, 118-121] Contamination of the mass spectrometer may be another serious disadvantage of direct analysis.[68, 73] It is often necessary, therefore, to include a sample preparation step to reduce matrix effects, lower the limits of detection, improve linearity, bring selectivity to the analysis, and enable the analysis of large batches without deterioration of instrument performance. Established sample preparation procedures have been used for this purpose: liquid extraction to detect steroid esters in hair[122] and lipids in lung tissue[123] by DESI, hydrolysis and solid phase extraction to enhance the DAPPI analysis of drugs of abuse in urine,[73] hydrolysis and liquid–liquid extraction to enable the DESI analysis of drugs and their metabolites in urine,[27] protein precipitation and derivatization to detect sera metabolic profiles by DART,[124, 125] liquid extraction and SPE purification to quantify mycotoxins in cereal by DART[111] and detect pesticides in fruit by DESI,[126] and liquid-phase microextraction to analyze basic drugs from urine by DESI.[127] Direct open air surface sampling/ionization MS also enables the direct study on the separation or extraction material. Analytes have been studied directly on TLC plates,[15, 104, 128-132] but also on solid-phase extraction cartridges,[133] fibers,[134] films,[135] membranes,[136] and single-drop liquid microextraction droplets.[137]

The ability of direct open air surface sampling/ionization MS methods to sample finely localized spots on surfaces has also allowed them to be applied in mass spectrometry imaging (MSI, Table 3).[138] In MSI, adjacent areas of a surface are analyzed in a systematic manner, and the measured spectra are combined into a series of images that show the location-dependent intensities of the studied ions. Because MSI can simultaneously detect and distinguish hundreds or even thousands of molecules with good sensitivity, it offers a unique view of the sample unobtainable by other imaging techniques, such as immunostaining, spectroscopy imaging, magnetic resonance imaging, or positron emission tomography. MALDI[6, 139] and SIMS,[140] which traditionally are used for MSI, offer spatial resolution at sub-cellular scale (starting from ~600 nm[141] and ~50 nm,[142] respectively). However, the vacuum environment of MALDI and SIMS is a disadvantage for *in vivo* analyses, and the matrix can cause background at low m/z (< 500). Utilizing direct open air surface sampling/ionization MS by combining desorption with a heated atomic force microscopy (AFM) tip and ionization by ESI, Ovchinnikova *et al.*[143] recently achieved sampling of spots with ~250 nm diameter. MSI of real samples has not yet been demonstrated. In direct open air surface sampling/ionization MSI (Table 3) a sampling spot size of tens of microns has been achieved for polar lipids and small polar analytes. DAPPI-MSI[99] has been demonstrated for the low polarity analytes cholesterol, carnosol, and tocopherol, but the spatial resolution was worse than what can be achieved for polar compounds by DESI and LAESI, for example.

Table 3. *Direct open air surface sampling/ionization MS methods used for mass spectrometry imaging, and selected applications.* uses fs pulse length laser, while other laser sources use ns pulse lengths.*

Method	Sample	Examples of analytes	Spot size (lateral resolution)	Ref
DESI	rat brain tissue section	phospholipids, fatty acids	<500 μm	144
	TLC plate	rhodamine dyes	~400 μm	130
	tissue section	clozapine and its metabolites	~245 μm	145
	tissue section	phospholipids, fatty acids	~35 μm	146
reactive DESI	rat brain section	cholesterol (betaine aldehyde reagent)	~200 μm	98
LAESI	*A. squarrosa* leaf	methoxykaempferol glucuronide	~350 μm	89
	rat brain tissue section	choline, phospholipids	~200 μm	147
	onion bulb scale	cyanidin	cell-by-cell (~40 μm)	91
ELDI	dry fungi	2, 4, 5-trimethoxybenzaldehyde, triterpenoids	100 μm×150 μm	148
DAPPI	mouse brain tissue section	cholesterol	~1 mm	99
	sage leave	carnosol, tocopherol		
IR-LAMICI	pharmaceutical tablet	acetaminophen	~300 μm	36
LDI	onion epidermis cells	glucose	10 μm	149*
LA-FAPA	pharmaceutical tablet	acetaminophen, caffeine	~10-300 μm	40
	image printed on paper	caffeine (doped to ink)		
	wet turkey tissue (luncheon meat)	lidocaine (spiked on top of the tissue)		

2 AIMS OF THE STUDY

The overall aim of the study was to develop and apply direct open air surface sampling/ionization mass spectrometry methods in the study of neutral and nonpolar compounds.

Specifically, the aims of the research were

- to compare commercially available direct and alternating current krypton discharge vacuum ultraviolet lamps for more efficient photoionization in μAPPI and DAPPI ion sources (I)

- to reduce matrix effects and improve sensitivity of DAPPI-MS analyses of complex aqueous samples by developing a PDMS extraction phase that can be analyzed directly by DAPPI-MS (II)

- to develop a direct open air surface sampling/ionization mass spectrometry method with improved spatial resolution for the study of neutral and nonpolar compounds (III)

- to assess the feasibility of laser ablation atmospheric pressure photoionization in mass spectrometry imaging by studying the distribution of phytochemicals on sage leaves (IV)

- to develop an ambient ionization method with high ionization efficiency for both nonpolar and polar compounds by utilizing heat-assisted laser ablation electrospray ionization (V).

3 EXPERIMENTAL

This section briefly describes the materials, instrumentation, and ion source setups of the study. Details are provided in the original publications (I-V).

3.1 CHEMICALS, MATERIALS, AND SAMPLES

The chemicals that were used are listed in Table 4 and the samples that were analyzed in Table 5.

Table 4. *Chemicals used in the study.*

Chemical	Manufacturer/supplier	Note	Publication
1,1′,2,2′-tetramyristoyl cardiolipin (TMCL)	Avanti Polar Lipids, Alabaster, AL	standard	V
1,2-dioleoyl-*sn*-glycero-3-phosphocholine	Sigma-Aldrich, St. Louis, MO	standard	V
1,4-dinitrobenzene	Aldrich, Milwaukee, WI	standard	I
1-palmitoyl-2-oleoyl-*sn*-glycerol (DG(34:1), 2 mg/mL in chloroform)	Avanti Polar Lipids, Alabaster, AL	standard	V
2-naphthoic acid	Aldrich, Milwaukee, WI	standard	I
acetaminophen	Merck, Darmstadt, Germany	standard	I, II
acetone	Merck, Darmstadt, Germany	solvent	I
	Mallinckrot Baker B.V., Deventer, The Netherlands	solvent	II
anisole	Fluka Chemie GmbH, Buchs, Switzerland	solvent	II
	Sigma-Aldrich, St. Louis, MO	solvent	III, IV
anthracene	Fluka Chemie GmbH, Buchs, Switzerland	standard	I, II
benzo[*a*]pyrene	Sigma-Aldrich, Steinheim, Germany	standard	I, II
bradykinin fragment 1-8 acetate hydrate	Sigma-Aldrich, St. Louis, MO	standard	III, V
cholecalciferol	Sigma-Aldrich, St. Louis, MO	standard	III, V
cholesterol	Alfa Aesar, Ward Hill, MA	standard	III, V
dehydroepiandrosterone (DHEA)	Sigma-Aldrich, St. Louis, MO	standard	III, V
diisopropylamine	Fluka Chemie GmbH, Buchs, Switzerland	solvent	II
estrone	Sigma-Aldrich, St. Louis, MO	standard	III, V
fluorescein	Riedel-de Haen (Sigma-Aldrich, Seelze, Germany)	standard	II
formic acid	Fluka, Seelze, Germany	modifier	V
fucose	Sigma-Aldrich, St. Louis, MO	standard	V
glyceryl trioctanoate (tricaprylin)	Sigma-Aldrich, St. Louis, MO	standard	III, V
hexane	VWR international, Espoo, Finland	solvent	I, II
lysozyme from chicken egg white	Sigma-Aldrich, St. Louis, MO	standard	V

Table 4 continued *Chemicals used in the study.*

Chemical	Manufacturer/supplier	Note	Publication
methanol	Fluka Chemie GmbH, Buchs, Switzerland	solvent	I
	Mallinckrodt Baker B.V., Deventer, The Netherlands	solvent	II
	Sigma-Aldrich, St. Louis, MO	solvent	III
	Fluka, Seelze, Germany	solvent	V
midazolam	Hoffman-La Roche, Basel, Switzerland	standard	I, II
naphtho[2,3-*a*]pyrene	Sigma-Aldrich, St. Louis, MO	standard	V
nicotine	Alfa Aesar , Karlsruhe, Germany	standard	I, II
nitrogen	GTS-Welco, Inc., Allentown, PA	nebulizer gas	III-V
pentane	Lab-Scan Analytical Sciences, Dublin, Ireland	solvent	II
perylene	Sigma-Aldrich, St. Louis, MO	standard	V
pyrene	Sigma-Aldrich, St. Louis, MO	standard	V
testosterone	Sigma-Aldrich, Steinheim, Germany	standard	I, II
toluene	Sigma-Aldrich, Steinheim, Germany	solvent	I, II
	Sigma-Aldrich, St. Louis, MO	solvent	III, V
triethylamine	Sigma-Aldrich, Steinheim, Germany	solvent	II
verapamil hydrochloride	Aldrich, Milwaukee, WI, USA	standard	I, II
	Sigma-Aldrich, St. Louis, MO	standard	III, V
water (HPLC grade)	Ricca Chemical Company, Arlington, VA	solvent	III
	Alfa Aesar, Ward Hill, MA	solvent	V
water (Milli-Q)	Millipore, Molsheim, France	solvent	I, II
α-tocopherol	Sigma-Aldrich, St. Louis, MO	standard	III

The spray solvent for LAESI and HA-LAESI was prepared by mixing equal volumes of water and methanol and adding 0.1% HCOOH. Stock solutions of the standards (1-10 mM or 1-5 mg/mL) were prepared in toluene (PAHs), water (nicotine, lysozyme, bradykinin fragment 1-8, and fucose) or methanol (all other standards). In the micro APPI (μAPPI) experiments (I), 1 and 10 μM working mixtures of the analytes were prepared in the six studied μAPPI solvents and introduced to the source by direct infusion. In the DAPPI (I, II), LAAPPI (III, V), LAESI (V), and HA-LAESI (V) experiments, the working solutions were prepared in water/methanol (1:1, v:v) except for bradykinin 1-8, which in III was diluted in water. In LAAPPI, LAESI, and HA-LAESI, 0.5-10 μL of the standard working solution was pipetted onto a concave microscope glass slide and analyzed as a liquid droplet. In DAPPI (I), 1 μL of the working solution was applied on the poly(methyl methacrylate) (PMMA) surface (Vink Finland Oy, Kerava, Finland), left to dry, and analyzed directly on the PMMA surface. In study II, spiked analytes from 3 mL-1 L aqueous samples were extracted onto polydimethylsiloxane (PDMS) slides (approx. 1 mm×7 mm×10 mm) and the slides were analyzed by DAPPI-MS. The slides were prepared as follows: PDMS base and curing agent (Sylgard 184 PDMS elastomer kit, Dow Corning GmbH, Wiesbaden, Germany) were weighed and thoroughly mixed. Air bubbles were removed in a vacuum. The solution was cast on a glass plate and cured on a hotplate. The cured PDMS was cut to measure.

Table 5. *Samples investigated and sample preparation methods employed.*

Sample	Supplier/source	Sample preparation	
wastewater	Finnish Environment Institute	100 mL aliquot spiked with anthracene, verapamil, and testosterone (100nM each), extracted into PDMS	II
urine	volunteer	3 mL aliquot spiked with acetaminophen, nicotine, anthracene, benzo[*a*]pyrene, midazolam, verapamil, fluorescein, and testosterone (1 µM each), extracted into PDMS	II
sour orange (*Citrus aurantium)* leaves	USDA Agricultural Research Service Subtropical Agricultural Research Center	particulates wiped from surface and analyzed without further sample preparation	III
rat brain	National Institutes of Health (USA)	cryosectioned into 200 µm thickness, analyzed without further sample preparation	III
sage (*Salvia officinalis*) leaves	local supermarket	analyzed as such	IV
mouse brain	Children's National Medical Center (USA)	embedded in OCT compound and cryosectioned into 40 µm thickness, analyzed without further sample preparation	V
avocado (*Persea americana)* fruit	local supermarket	pulp cut into 0.5 mm thick sections and analyzed without further sample preparation	V
pansy (*Viola*) petals	local supermarket	analyzed as such	V

3.2 INSTRUMENTATION

Table 6 lists the most important commercial instruments used in the study; the notes indicate their use. In-house built and modified instruments were also employed. Those of greatest importance were the Peltier cooling stage, built with a ceramic thermoelectric module (Ferrotec Corp., Bedford, NH), which was used to cool samples (III-V), and the modified ARC VM-502VUV spectrometer (Acton Research Corporation, Acton, MA), which was used to record the emission spectra of the UV lamps (I).

Table 6. *Commercial instruments used in the study.*

Instrument/equipment (model)	Manufacturer/supplier	Note	Publication
ion trap mass spectrometer (6330)	Agilent Technologies, Santa Clara, CA	mass analysis	I, II
AccuTOF mass spectrometer (JMS-T100LC)	JEOL Ltd., Peabody, MA	mass analysis	III-V
dc krypton discharge photoionization lamp (PKS 100)	Heraeus Noblelight, Cambridge, UK	APPI	I, II
rf krypton discharge photoionization lamp (PKR 100)	Heraeus Noblelight, Cambridge, UK	APPI	I, III-V
Nd:YAG OPO laser	Vibrant IR, Opotek, Carlsbad, CA	sample ablation	III-V
syringe pump (PHD 2000)	Harvard Apparatus, Holliston, MA	sample/spray solvent delivery	I, II
syringe pump (Physio 22)	Harvard Apparatus, Holliston, MA	spray solvent delivery	III-V
syringe pump (SP100I)	World Precision Instruments Inc., Sarasota, FL	ES solvent delivery	V
mass flow controller (GFC17)	Aalborg, Orangeburg, NY	spray gas regulation and flow measurement	I, II, IV, V
panel-mounted single flow tube	Aalborg, Orangeburg, NY	spray gas flow measurement	III
dc power supply (ISO-TECH 603)	RS Components, Northants, U.K.	microchip heating	I, II
dc power supply (HY3005)	RSR Electronics, Rahway, NJ	microchip heating	III-V
dc high voltage power source (PS350)	Stanford Research Systems Inc., Sunnyvale, CA	ES high voltage generator	V
infrared thermometer (845)	Testo Inc., Sparta, NJ	temperature measurement	III-V
shaker (Multi Reax)	Heidolph Instruments, Schwabach, Germany	sample agitation	II
hotplate (Stuart Scientific SH3D)	Bibby Sterilin, Staffordshire, United Kingdom	PDMS curing	II

3.3 ION SOURCES

Different home-built mass spectrometer ion sources were used in the work. In I, direct current (dc) and radio frequency (rf) alternating current photoionization lamps were compared with μAPPI (Figure 2) and DAPPI (Figure 1). The μAPPI source was originally described by Kauppila *et al.*[150] An μAPPI source built on the same principal design was used in this study, but instead of the original diagonal geometry, an on-axis spray with orthogonal lamp-to-spray geometry was preferred to help positioning of the UV lamps in an identical manner. The DAPPI source was introduced by Haapala *et al.*[35] in 2007, and it was used with only minor modifications to the original design (I, II).

The LAAPPI and HA-LAESI ion sources, shown in Figures 3 and 4, respectively, were developed as part of the research (publications III and V, respectively). In both

ion sources, the sample is placed in front of the MS inlet, ca. 8-15 mm below it, and the sample surface is ablated by the mid-infrared (mid-IR) laser. In LAAPPI, the ablated projectiles are intercepted with a hot solvent jet directed to the MS inlet, and the mixed sample and solvent plumes are irradiated with the rf krypton discharge photoionization lamp. In HA-LAESI, the projectiles are intercepted with electrospray and hot nitrogen jet, which are directed at the MS inlet in the geometry presented in Figure 4. In V, the new LAAPPI and HA-LAESI sources were compared with the previously introduced LAESI source[38] (Figure 5).

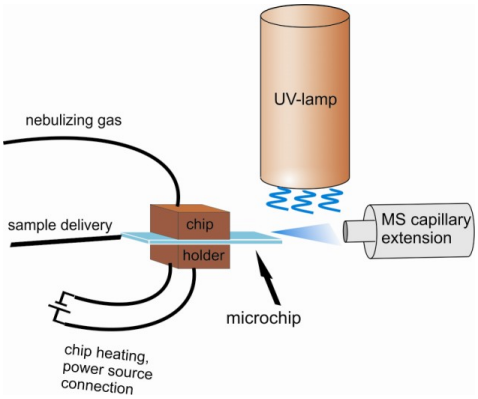

Figure 2 Schematic presentation of the µAPPI ion source.

All sources except the LAESI utilize custom-made heated nebulizer microchips designed and manufactured in collaboration between the Division of Pharmaceutical Chemistry at the University of Helsinki, Prof. Sami Franssila's group at Aalto University, and Micronova (Espoo, Finland). The manufacturing of the microchips[151] and the microchip holder[63] have been described in detail previously. In this work, the nebulizer microchips were used to vaporize the sample (I) or to provide a heated, confined jet of solvent vapor (I-V) or a narrow stream of hot gas (V). The temperature of the heated jet can be chosen by changing the microchip heating power; the maximum jet temperature is approx. 350 °C. The solvent and nebulizer gas flow rates and estimates of the applied temperatures are given in the original publications (I-V).[152]

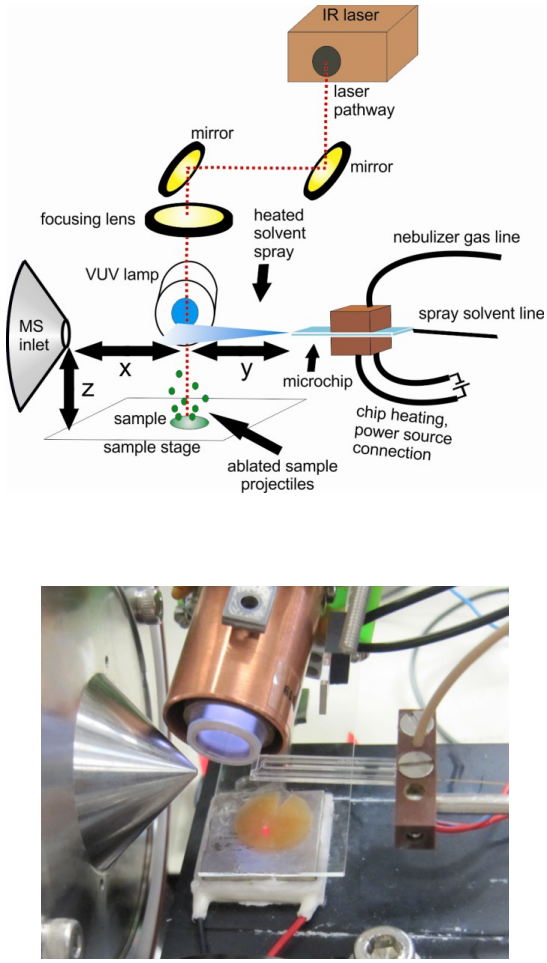

Figure 3 A schematic presentation (top) and a photograph (bottom) of the LAAPPI ion source.

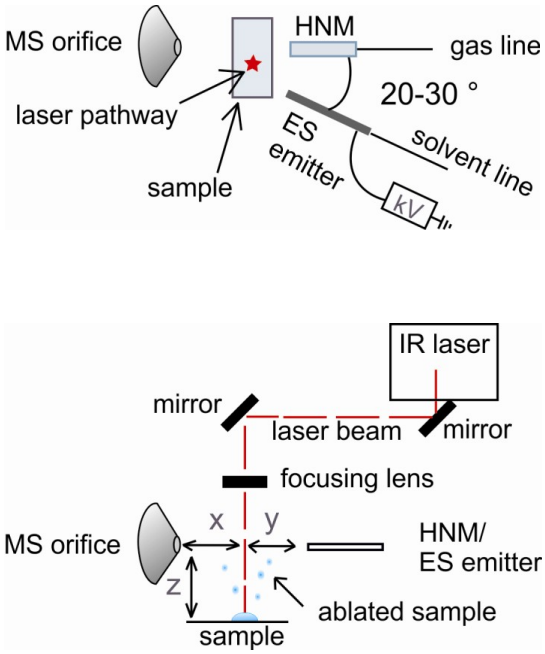

Figure 4 The HA-LAESI source seen from the top (top) and from the side (bottom). HNM = heated nebulizer microchip.

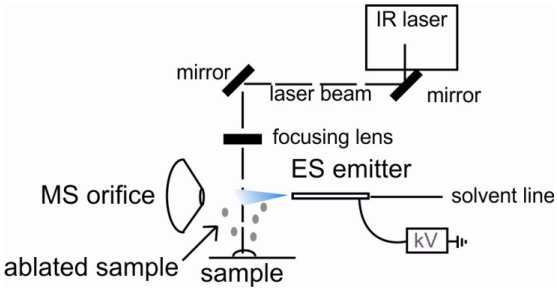

Figure 5 A schematic representation of the LAESI ion source.

4 RESULTS AND DISCUSSION

This section summarizes and discusses the results of the research. Details are provided in the original publications (I-V).

4.1 COMPARISON OF DIRECT AND ALTERNATING CURRENT VACUUM ULTRAVIOLET PHOTOIONIZATION LAMPS

Commercially available direct current (dc) and radio frequency (rf) alternating current krypton discharge vacuum ultraviolet lamps were compared with the purpose of improving the efficiency of the DAPPI ion source, and explaining discrepancies in the performance of the commercial APPI ion sources. The UV emission spectra of the lamps were measured and the performance of the lamps was compared in μAPPI-MS and DAPPI-MS. Because the APPI ionization process depends on the used solvents,[61, 64, 67, 153, 154] six different solvent compositions were studied in μAPPI and five spray solvents in DAPPI. In addition, completely solvent-free DAPPI was explored.

UV emission spectra

Measurement of the UV emission spectra of the dc and rf vacuum ultraviolet lamps showed the relative intensities of the 10.0 and 10.6 eV photons to be on the same level with both lamps (approximately 7:1, Figure 6a). However, the emission distributions along the diameter of the lamp exit window showed the beam of the rf lamp to be wider than that of the dc lamp (Figure 6b). The broader width results in a larger efficient ionization area and a significantly larger number of photons, corresponding to a total photon flux about five-fold that of the dc lamp.

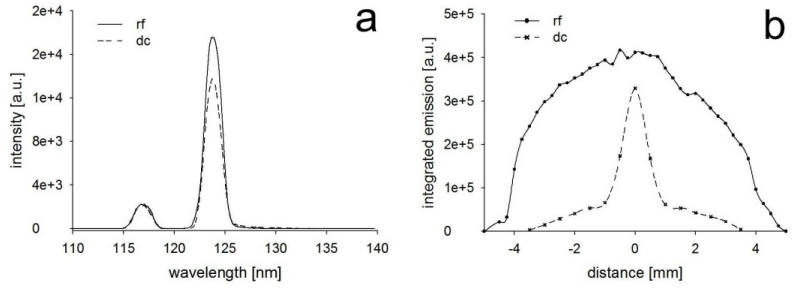

Figure 6 Emission spectra of the dc and rf lamps (a) and total integrated intensity of the 10.0 and 10.6 eV photons emitted by the dc and rf lamps plotted as function of the lamp window position (b).

Positive ion mode

Solvent ions can act as reactants in the ionization reactions of analytes (see sect. 1.1.3).[61] The solvent ions produced by the dc and rf lamps were studied with the μAPPI and DAPPI sources in positive ion mode for six different solvents. The solvent ions observed with the μAPPI source are listed in Table 7. Except for toluene, the solvent spectra were similar for the two lamps: the ions at *m/z* 108 and 199, probably oxidation products of toluene,[155] were seen only with the rf lamp. In both techniques, solvents with low ionization energy (toluene, acetone) produced high reactant ion abundances, while methanol and water, whose IEs are above the energy of the UV lamp photons, showed low reactant ion intensities (Figure 7a). With both techniques and all solvent systems, the rf lamp showed a larger total number of reactant ions than the dc lamp. The effect was most prominent with methanol and methanol/water (1:1), where the total reactant ion signal was an order of magnitude higher with the rf lamp in μAPPI and the reactants were not detected at all in DAPPI with the dc lamp. Since there were no differences in the energies of the photons emitted by the two lamps, the larger number of reactant ions formed by the rf lamp must be due to the larger efficient ionization area associated with the broader light beam and the larger total amount of photons emitted by the rf lamp.

Table 7. *The studied solvent compositions, gas-phase properties of the solvents, and observed reactant ions in positive ion μAPPI. The 10 most abundant ions with relative intensity ≥ 10% and S/N ≥ 3 in m/z range 20-148 are reported for acetone, hexane, methanol, methanol/water, and methanol/toluene. For toluene, ions in the range m/z 20-400 are reported. IE = ionization energy, PA = proton affinity, S = solvent.*

Solvent composition	**Gas-phase properties of the solvent(s)[62]**		**Observed reactant ions (*m/z*, suggested identity and relative abundance in parenthesis)**	
	IE (eV)	PA (kJ/mol)	dc lamp	rf lamp
toluene	8.8	784.0	92 ($S^{+\cdot}$, 100), 106 (25)	92 ($S^{+\cdot}$, 100), 106 (20), 108 ($[S+O]^+$, 10), 199 (12)
acetone	9.7	812.0	43 (10), 59 ($[S+H]^+$, 68), 99 (100), 117 ($[2S+H]^+$, 86)	43 (10), 59 ($[S+H]^+$, 70), 99 (100), 117 ($[2S+H]^+$, 86)
hexane	10.1		43 (23), 55 (22), 57 (21), 83 (47), 85 ($[S-H]^+$, 100), 97 (18), 99 (38), 101 (55), 115 (83), 117 (24)	43 (20), 55 (17), 57 (20), 83 (38), 85 ($[S-H]^+$, 100), 99 (21), 101 (33), 115 (10), 117 (10)
methanol	10.8	754.3	33 ($[S+H]^+$, 64), 63 (29), 65 ($[2S+H]^+$, 20), 73 (19), 87 (34), 103 (18), 121 (47), 129 (37), 140 (100), 141 (22)	33 ($[S+H]^+$, 73), 47 (55), 65 ($[2S+H]^+$, 55), 73 (47), 87 (100), 101 (37), 121 (18), 129 (22), 136 (23), 140 (34)
methanol (S_1)/water (S_2) (1:1)	10.8/ 12.6	754.3/ 691.0	33 ($[S_1+H]^+$, 100), 47 (82), 59 (14), 65 ($[2S_1+H]^+$, 91), 73 (41), 87 (42), 101 (21), 117 (13), 133 (19), 135 (12)	33 ($[S_1+H]^+$, 100), 47 (62), 65 ($[2S_1+H]^+$, 75), 73 (30), 87 (37), 101 (16), 115 (12), 117 (11), 136 (23), 141 (13)
methanol (S_1)/ toluene (S_2) (9:1)	10.8/ 8.8	754.3/ 784.0	33 ($[S_1+H]^+$, 89), 47 (56) 65 ($[2S_1+H]^+$, 72), 73 (57), 87 (100), 93 ($[S_2+H]^+$, 68), 101 (41), 107 (56), 139 (59), 141 (33)	33 ($[S_1+H]^+$, 100), 47 (60), 65 ($[2S_1+H]^+$, 81), 73 (57), 87 (99), 93 ($[S_2+H]^+$, 73), 101 (44), 107 (46), 125 (47), 139 (36)

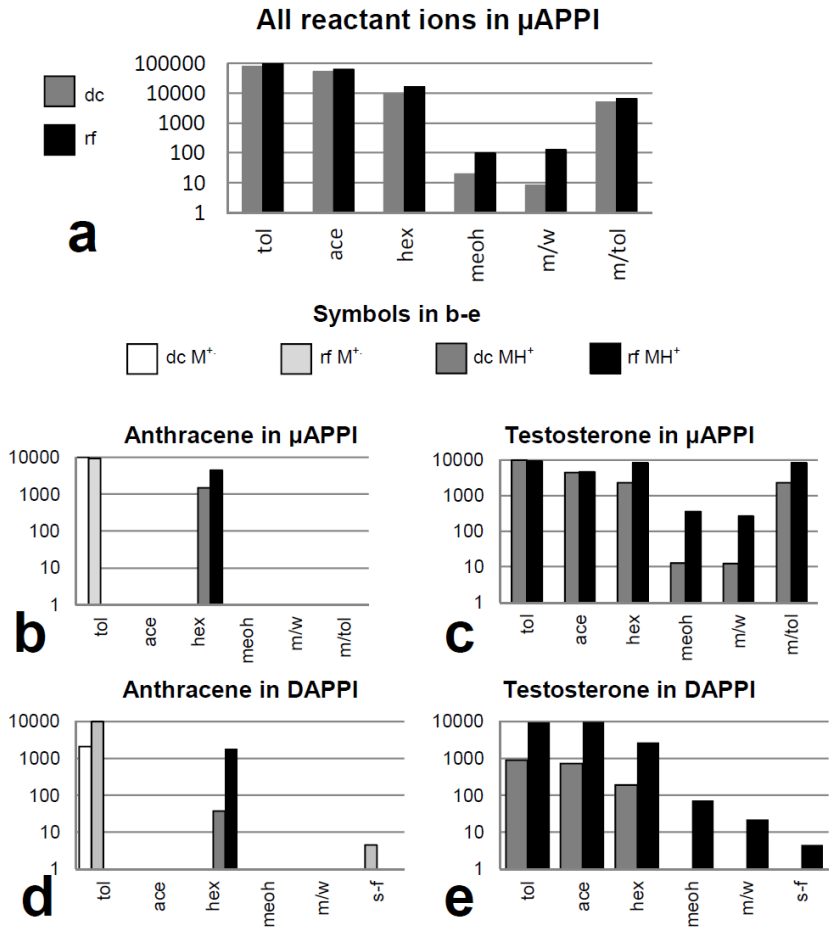

Figure 7 Comparison of ionization efficiency with µAPPI and DAPPI in positive ion mode with different solvents and the rf and dc lamps. a) Relative signal intensity of all reactant ions in µAPPI at *m/z* 20-148. The values for the different solvents should be compared with caution since the mass spectrometer discriminates against low *m/z* ions. b, c) Relative signal intensities of anthracene $M^{+\cdot}$ and MH^+ and testosterone MH^+ ions measured by µAPPI, and d, e) average relative areas of the spot signals of anthracene $M^{+\cdot}$ and MH^+ and testosterone MH^+ ions measured by DAPPI. In µAPPI the analyte concentration was 1 µM each, in DAPPI the analyte amount was 10 pmol each. tol = toluene, ace = acetone, hex = hexane, meoh = methanol, m/w = methanol/water (1:1, v:v), m/tol = methanol/toluene (9:1, v:v), s-f = solvent-free DAPPI.

Next, the formation of analyte ions was investigated for the dc and rf lamps with a mixture of acetaminophen, anthracene, benzo[*a*]pyrene, midazolam, nicotine, testosterone, and verapamil. The analyte ions that formed depended on the used solvent(s), but were the same for the two lamps in µAPPI. In DAPPI the dc lamp did not produce analyte ions when methanol and methanol/water were used as spray

solvents nor when there was no spray solvent at all. Otherwise the two lamps produced the same analyte ions.

When toluene was used as the solvent, analytes with low IEs (anthracene, benzo[*a*]pyrene, midazolam) produced $M^{+\cdot}$ ions via charge exchange (Reaction 3, Scheme 2), whereas those with high PAs (midazolam, testosterone, and verapamil) produced MH^+ ions, probably by proton transfer from $M^{+\cdot}$ ions of toluene (Reaction 4, Scheme 2). The solvents that produced MH^+ or $[M-H]^+$ reactant ions (acetone, methanol, methanol/water (1:1), methanol/toluene (9:1), and hexane) mainly produced abundant protonated molecules of the analytes, most likely formed via proton-transfer reactions between the protonated solvent and the analyte (Reaction 6, Scheme 2). The ionization behavior of the solvents is in agreement with previous reports on DAPPI[60] and APPI.[61] Solvent-free DAPPI with the rf lamp produced analyte $M^{+\cdot}$ ions, possibly by direct photoionization (Reaction 1, Scheme 2), and MH^+ ions by proton or hydrogen transfer (Reactions 4-6, Scheme 2). The proton- or hydrogen-donating species could not be identified, however.

The ionization efficiencies of the dc and rf lamps for analytes were closely similar to those observed for the solvent reactant ions. Results for testosterone and anthracene with μAPPI and DAPPI are presented in Figure 7b-e. The lamps were also compared in DAPPI-MS/MS mode by determining the limits of detection (LOD) for nicotine, midazolam, testosterone, and verapamil with acetone as the DAPPI spray solvent. The LODs determined with the dc lamp were 1.5–5 fold those obtained with the rf lamp. Clearly, the rf lamp provides more efficient analyte ionization than the dc lamp, especially in low IE solvent systems. It was suspected that the higher photon flux of the rf lamp leads to greater production of reactant ions, which allows more efficient ionization of the analytes.

Negative ion mode

The ionization of 1,4-dinitrobenzene, acetaminophen, and 2-naphthoic acid was studied in negative ion mode, with the same solvents as used in positive ion mode. The same ions were observed for each analyte in μAPPI and DAPPI, independent of the solvent and lamp. 1,4-Dinitrobenzene produced negative molecular ions ($M^{-\cdot}$) and a fragment ion $[M-NO]^-$ at *m/z* 138. The analytes acetaminophen and 2-naphthoic acid, which contain acidic groups, produced deprotonated molecules ($[M-H]^-$). Since 1,4-dinitrobenzene has high electron affinity, it is probably ionized by charge-exchange reaction with $O_2^{-\cdot}$ (Reaction 8, Scheme 2) or by electron capture (Reaction 7, Scheme 2). Acetaminophen and 2-naphthoic acid are probably deprotonated by $O_2^{-\cdot}$ (Reaction 9, Scheme 2).

Examination of the effect of the solvents in negative ion μAPPI showed the dc and rf lamps to produce analyte ions most efficiently with acetone and toluene as solvents (Figure 8). The ionization efficiency was over an order of magnitude higher than with methanol (IE for methanol is 10.8 eV and for methanol dimer 9.8 eV).[156] It is likely, therefore, that the ionization efficiency of the analyte depends on the photoionization efficiency of the solvent, because photoionization of the solvent and the production of thermal electrons were more efficient with the solvents with lower IE (toluene, acetone) than those with higher IE (hexane, methanol).

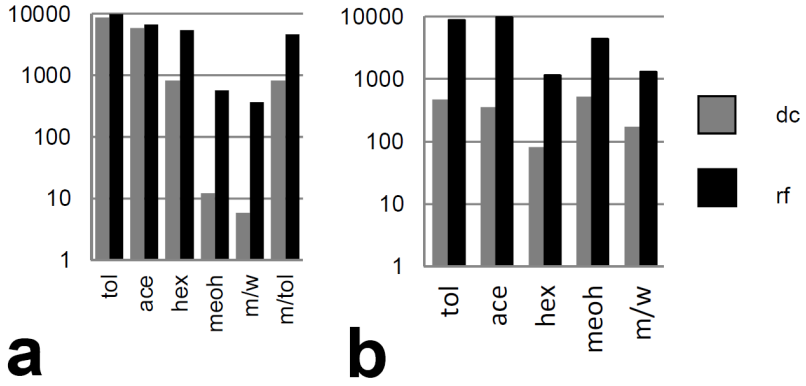

Figure 8 The relative intensity of 1,4-dinitrobenzene (10 µM) $M^{-\bullet}$ in µAPPI (a), and the average relative area of the spot signal of 1,4-dinitrobenzene (10 pmol) $M^{-\bullet}$ in DAPPI (b) measured with the dc and rf lamps. Abbreviations: tol = toluene, ace = acetone, hex = hexane, meoh = methanol, m/w = methanol/water (1:1), m/tol = methanol/toluene (9:1).

In negative as in positive ion mode, the rf lamp provided higher ionization efficiency than the dc lamp in both µAPPI and DAPPI (Figure 8). Because the rf lamp provides larger ionization area and emits a larger number of photons, it probably also provides more efficient photoionization of the solvent. This leads to the formation of a larger number of the thermal electrons needed for the ionization of the analytes and may explain the better ionization efficiency of the rf lamp. The broader light beam of the rf lamp might also cause more efficient release of electrons from the metal surfaces of the ion source.

4.2 DESORPTION ATMOSPHERIC PRESSURE PHOTOIONIZATION WITH POLYDIMETHYLSILOXANE AS EXTRACTION PHASE AND SAMPLE PLATE MATERIAL

As noted above (sect. 1.2), matrix effects can be a severe disadvantage in direct open air surface sampling/ionization MS analyses. Therefore a sample preparation method for the DAPPI-MS analysis of neutral and nonpolar compounds was developed. Polydimethylsiloxane (PDMS), a widely used solid-phase extraction material, was chosen as the extraction phase because it is hydrophobic and thus well suited for the target analytes. PDMS has previously been used in stir bar sorptive extraction[157, 158] and solid-phase microextraction.[159] Here the DAPPI analysis was performed directly on the PDMS extraction phase, without a separate elution step.

Method optimization

With use of the native PDMS polymer as extraction material, abundant oligomers ($[[Si(CH_3)_2O]_n+H]^+$) appeared in the DAPPI-MS spectra. A means of reducing the background was accordingly sought, to avoid suppression and peak overlapping. Study was made of the manufacturing conditions of the PDMS polymer (variation of the ration of prepolymer to curing agent, and the curing time and temperature), but no major effect on the DAPPI-MS background was observed. Because certain solvents reportedly cause PDMS to swell, and the swelling ability has been linked to the extraction of oligomers from the cured PDMS polymer,[160] the effect of swelling of PDMS was studied in acetone, toluene, hexane, pentane, triethylamine, and diisopropylamine (Figure 9). As expected from their greater swelling ability,[160] the two amines reduced the background most. The lower background might, however, also be due to reduced ionization efficiency of the polymer oligomers, since the solvent residues of the high PA amines could abstract protons from the protonated oligomer ions.

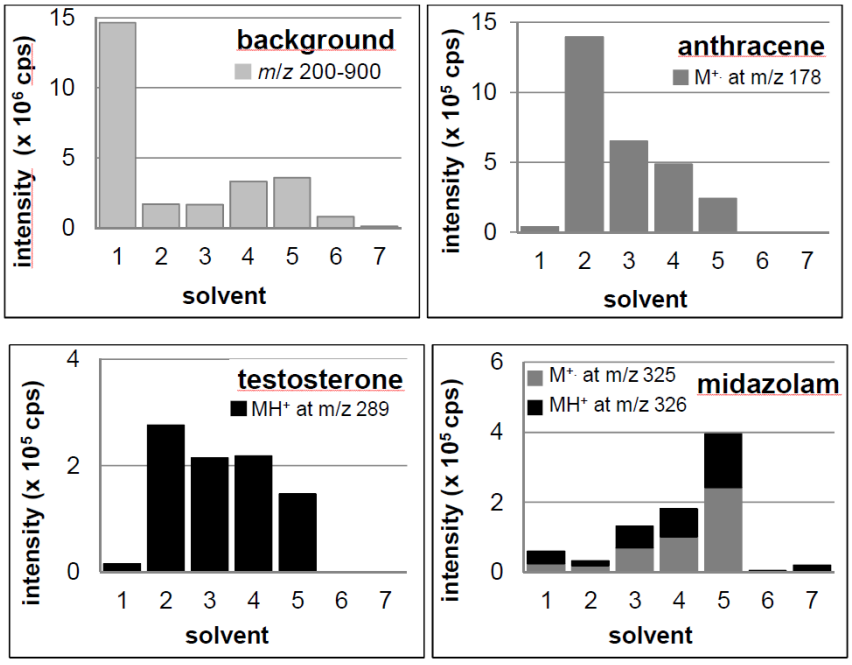

Figure 9 Effect of cleaning solvent on the background caused by PDMS and on the DAPPI-MS signals of anthracene, testosterone, and midazolam (10 µM each) extracted on the PDMS. The cleaning solvents were 1) no cleaning (native PDMS), 2) toluene, 3) hexane, 4) pentane, 5) acetone, 6) diisopropylamine, and 7) triethylamine. Toluene was the DAPPI spray solvent.

The cleaning solvent residues in PDMS might also affect the analyte ionization, since even small changes in solvent composition are reported to affect the ionization mechanism in APPI.[67] The effect of cleaning solvents in DAPPI was tested by

extracting acetaminophen, nicotine, anthracene, benzo[*a*]pyrene, midazolam, verapamil, fluorescein, and testosterone from aqueous 3 mL standard solutions to the cleaned PDMS (Figure 9). Acetaminophen and fluorescein were not detected with any of the cleaning agents, nor in the absence of a cleaning agent, probably because of the low extraction efficiency of acetaminophen (log $K_{o/w}$ = 0.27),[161] and low desorption and/or ionization efficiency of fluorescein. Toluene, hexane, pentane, and acetone did not affect the ionization process, as the same ions were observed for the analytes as with native PDMS. Anthracene, benzo[*a*]pyrene, nicotine, and testosterone were not detected when diisopropylamine or triethylamine was used as the cleaning solvent. Since the amines have high PAs (971.9 kJ/mol for diisopropylamine and 981.8 kJ/mol for triethylamine),[62] they compete for the ionization with these analytes. Verapamil and midazolam have high PAs, 980 and 1002 kJ/mol (both calculated),[162] respectively, and these analytes were protonated even in the presence of the amines. The results suggest that these amines could be used to provide selective extraction and ionization for the analysis of compounds with high PAs. A further observation was that the signals of anthracene, benzo[*a*]pyrene and testosterone were stronger when the PDMS was not dried after cleaning with toluene, hexane, or pentane (1.5- to 30-fold depending on the solvent and analyte). The straonger signals were attributed to the formation of a two-phase extraction medium and enhanced extraction by liquid–liquid partitioning of the analytes between the aqueous sample and the cleaning solvent inside the swelled PDMS. In light of the results, slides swelled with toluene were used in further studies.

The next step was to optimize the cleaning of PDMS and the extraction conditions. The background ion signals originating from the polymer were avoided by cleaning batches of five PDMS slides three times with 10 mL of toluene, each time for 1 h. Depending on the analyte, extraction times of 16–72 h were needed to reach the extraction equilibria. However 24 h extraction time was used for practical reasons. Although the equilibration times were long, parallel sample preparations enabled adequate MS analysis throughput. The extraction time could perhaps be reduced by further optimization of the extraction medium. Addition of organic modifier or salt to the sample did not significantly improve the extraction efficiency. The basic analytes—midazolam, verapamil, and nicotine—gave strongest signals when extracted in basic conditions (pH 14) because they are retained on the nonpolar PDMS most efficiently in their neutral form. When the sample volume was increased, the analyte ion intensities were increased up to 100 mL (testosterone and nicotine) and 200 mL (midazolam and verapamil). The subsequent levelling off of the signal was attributed to saturation of the extraction phase and competition between the analytes at the PDMS surface and depend on the analyte concentrations.

Finally, three different DAPPI spray solvents were tested. Anisole gave give a clean, low background even for native PDMS, while toluene and acetone produced the abundant oligomer peaks. The low background for anisole was attributed to the high PA of anisole radical cation, which prevented the efficient formation of protonated molecules of compounds with lower PA.[154] After the PDMS cleaning, the

three spray solvents gave similar background spectra. Toluene ionized the largest number of analytes, while acetone showed no peaks for the PAHs, and anisole did not ionize testosterone. The results suggest that the selectivity of the PDMS-DAPPI-MS method can be tuned through use of different spray solvents. Toluene was selected for futher work because of its suitability for the widest range of analytes. The optimized method was linear for ~1.5 decades (r^2 0.9815-0.9991) and gave LODs from 10-90 nM for 3 mL samples.

Applications

The optimized method was applied to the extraction and analysis of spiked wastewater and urine. Figure 10 presents a DAPPI-MS spectrum for 100 nM testosterone, anthracene, and verapamil extracted to PDMS from 100 mL of wastewater. The wastewater matrix did not give intense background ion signals in the studied *m/z* range of 50–600, but slightly elevated background and a weak suppression effect were observed when comparison was made with and identical analysis of spiked MilliQ-water. Anthracene and verapamil were detected in the wastewater MS scan spectra at the 100 nM concentration, but testosterone was observed only in the MS/MS spectrum, possibly because of binding to matrix components or because of lower extraction efficiency due to competition for extraction with the matrix species or the other spiked analytes.

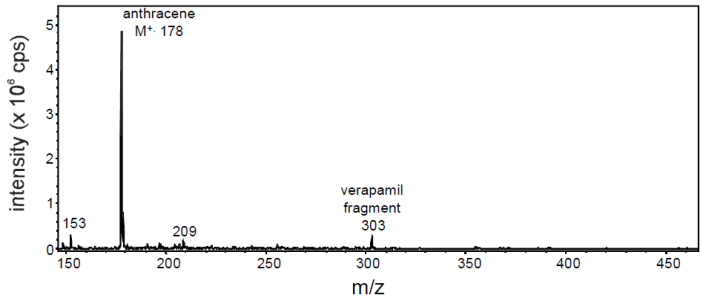

Figure 10 DAPPI-MS spectrum for 100 nM testosterone, anthracene, and verapamil extracted to PDMS from 100 mL of wastewater by the optimized PDMS method.

The urine sample was spiked with acetaminophen, nicotine, anthracene, benzo[*a*]pyrene, midazolam, verapamil, fluorescein, and testosterone at 1 µM concentration. The optimized PDMS-DAPPI-MS method was compared with direct DAPPI-MS analysis of the urine sample (1 µL applied on a PMMA plate). Spectra obtained by the two methods are presented in Figure 11. Nicotine ($[M+H]^+$), anthracene ($M^{+\cdot}$), benzo[a]pyrene ($M^{+\cdot}$), midazolam ($[M+H]^+$), verapamil ($[M+H]^+$ and a fragment at m/z 303), and testosterone ($[M+H]^+$) ions were observed when analytes were extracted onto and analyzed on PDMS. Anthracene, benzo[*a*]pyrene, and testosterone were not detected in the direct DAPPI analysis of the urine sample. The background was higher for the direct analysis. The signal intensities for

nicotine, verapamil and midazolam ions from PMMA were on the same level as the signals from PDMS, but depending on the analyte, the S/N was 2–10 times better for PDMS. Thus the developed method clearly improves the analysis of complex samples by DAPPI-MS.

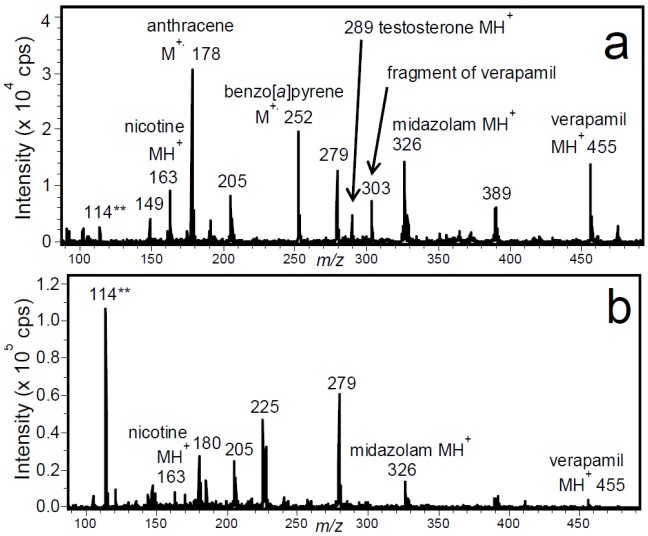

Figure 11 Analysis of urine spiked at 1 µM with acetaminophen, nicotine, anthracene, benzo[*a*]pyrene, midazolam, verapamil, fluorescein, and testosterone by a) PDMS-DAPPI-MS and b) direct DAPPI-MS.The sample volume was 3 mL in a and 1 µL in b. The ion marked with ** is possibly due to creatinine. Note the different scales.

4.3 INFRARED LASER ABLATION ATMOSPHERIC PRESSURE PHOTOIONIZATION MASS SPECTROMETRY

A laser ablation atmospheric pressure photoionization (LAAPPI) source was developed to enable study of neutral and nonpolar compounds at sub-mm spatial resolution (III). The MSI capabilities of LAAPPI were then demonstrated in a study of sage (*Salvia officinalis*) leaves (IV).

4.3.1 INFRARED LASER ABLATION ATMOSPHERIC PRESSURE PHOTOIONIZATION ION SOURCE

The LAAPPI ion source (Figure 3) was designed to sample the target by mid-IR laser ablation (2.94 µm, 5 ns, ~5-10 Hz) and ionize the analytes by photoionization. The operation of the ion source was tested with verapamil as the analyte. Verapamil was not detected when either the IR laser or the UV lamp was turned off, which

indicates, that the IR laser does not ionize the analyte. Furthermore, the sample was not desorbed by the hot spray solvent jet as occurs in DAPPI.[35] When the IR laser and the UV lamp were both turned on, the MH^+ ion of verapamil and a fragment at *m/z* 303 were detected.

Ionization mechanism of LAAPPI

The mechanism of atmospheric pressure photoionization is known from studies utilizing APPI[11, 12, 61, 154] and DAPPI.[35, 60] (A detailed discussion was presented in sect. 1.1.3 above). Because LAAPPI employs a UV lamp similar to that in APPI and DAPPI, it was considered that the same mechanisms would prevail in LAAPPI. In a study of the ionization, verapamil, DHEA, cholecalciferol, and estrone were analyzed using four different spray solvents (Table 8). Toluene, anisole and toluene/anisole (9:1, *v:v*) produced protonated molecules (MH^+) of verapamil and DHEA, which have relatively high PAs (calculated value of 980 kJ/mol for verapamil[162] and estimated value of 825 kJ/mol for DHEA[100]), and MH^+ and/or radical cation ($M^{+\bullet}$) of cholecalciferol and estrone, which have low IEs (estimated values 7.55[163] and 8.7 eV[164]). The relative abundances of the analyte $M^{+\bullet}$ ions were higher with anisole than with toluene, presumably because the PA of anisole (radical cation) is higher than that of toluene (radical cation). Charge exchange is therefore more favorable for anisole.[154] Only analyte MH^+ ions were observed when the toluene/methanol (1:9) mixture was used as the spray solvent. It was concluded, as described earlier for APPI,[61] that the toluene radical cation formed in photoionization (Reaction 2, Scheme 2) transfers a proton to methanol (cluster). Since the radical cation of toluene is then neutralized, charge exchange (Reaction 3, Scheme 2) is not possible. Analyte ionization can occur by proton transfer from the protonated methanol (cluster) to the analyte (Reaction 6, Scheme 2).

Table 8. *Analyte species observed with LAAPPI and different spray solvents.*

Spray solvent	**Observed ion species (*m/z*, relative intensity (%) in parenthesis; values for MH^+ ions have been corrected by reducing the natural abundance of the ^{13}C isotope of $M^{+\bullet}$)**			
	Verapamil	DHEA	Cholecalciferol	Estrone
Toluene	455 (100) MH^+, 303 (42)	289 (100) MH^+, 271 (62) $[MH\text{-}H_2O]^+$	384 (62) $M^{+\bullet}$, 385 (100) MH^+	270 (100) $M^{+\bullet}$, 271 (26) MH^+
Toluene/ methanol (1:9, *v:v*)	455 (100) MH^+	289 (100) MH^+, 271 (58) $[MH\text{-}H_2O]^+$, 253 (18)	385 (100) MH^+	271 (100) MH^+
Anisole	455 (27) MH^+, 303 (100)	289 (100) MH^+	384 (100) $M^{+\bullet}$, 385 (19) MH^+	270 (100) $M^{+\bullet}$
Anisole/ toluene (1:9, *v:v*)	455 (33) MH^+, 303 (100)	289 (100) MH^+	384 (100) $M^{+\bullet}$, 385 (32) MH^+	270 (100) $M^{+\bullet}$

Because the mid-IR laser ablation ejects the sample matrix to the ionization region of the LAAPPI source and samples were liquid solutions (methanol/water, 1:1, *v:v*) of the analytes, study was also made of the effect of the ablated sample solvent on the ionization process by monitoring solvent ions. Toluene was used as the spray solvent. Laser ablation of pure water led to decrease of ion intensities, but

there were no significant changes in the relative abundances of the ions. From this it was concluded that the flow of the ablated sample may reduce the flow of the spray solvent to the mass spectrometer by displacing it. When methanol/water was used as the sample, the intensities of protonated water and the radical cation of toluene decreased when the sample was ablated. The intensities of toluene $[C_7H_8+H]^+$ and methanol $[CH_3OH+H]^+$ and $[2CH_3OH+H]^+$ ions, in turn, increased. Evidently the water H_3O^+ and toluene $C_7H_8^{+\cdot}$ ions are neutralized in proton transfer to the ablated methanol or more probably to methanol clusters.[61] Thus, both the spray solvent and the sample solvent affect the ionization process in LAAPPI.

Quantitative performance of LAAPPI

The quantitative performance of LAAPPI was studied by determining the LODs, linearities, and repeatabilities for DHEA and verapamil. The concentrations of DHEA and verapamil at the LOD (S/N ≥ 3) were 5 µM and 0.25 µM, respectively. The smallest possible sample volume producing a signal was estimated to be 0.67 µl, and absolute LODs of 3.3 pmol and 170 fmol were calculated for DHEA and verapamil, respectively. A similar concentration at LOD has been reported for verapamil in LAESI,[38] and the estimated absolute LOD of verapamil is similar to what was estimated for acetaminophen in IR-LAMICI.[36] The correlation coefficients (r^2) of the calibration curves plotted on log-log scales from LODs to 1 mM were 0.99, indicating adequate linearity. The relative standard deviations at 100 µM for four DHEA and verapamil samples were 25% and 27%, respectively. LAAPPI is concluded to be semiquantitative.

Applications

The feasibility of LAAPPI in real applications was assessed by studying the LAAPPI-MS fingerprints of *Citrus aurantium* leaves and rat brain tissue with toluene as the spray solvent. Two types of spectra were obtained from single *Citrus aurantium* leaves. Most of the spectra showed ions predominantly below *m/z* 300 (Figure 12a). Probably these originated from volatile terpenes[165, 166] and other leaf metabolites. For example, the ion at *m/z* 196.15 could be the $M^{+\cdot}$ of linalyl acetate and that at *m/z* 153.13 the $[M-H]^+$ of linalool. Both these compounds are abundant in a common chemotype of *Citrus aurantium*.[165] Some of the spectra also showed abundant ions at *m/z* 340-420 (Figure 12b). The masses of some of these ions correspond to previously reported[167] phytochemicals of *Citrus aurantium*: *m/z* 373.13, 389.13, 403.14, and 419.14 ions might be due to MH^+ of tangeritin (calculated *m/z* 373.128, Δ*m/z* 0.007), 5-demethyl nobiletin (calc. *m/z* 389.123, Δ*m/z* 0.006), nobiletin (calc. *m/z* 403.139, Δ*m/z* -0.004), and natsudaidain (calc. *m/z* 419.134, Δ*m/z* 0.004), respectively. The nonpolar structures of these compounds suggest that they are stored in the oil glands[168] of the leaf. Since only some of the spots gave spectra with these signals, the respective ions may be due to ablation of the scattered glands.

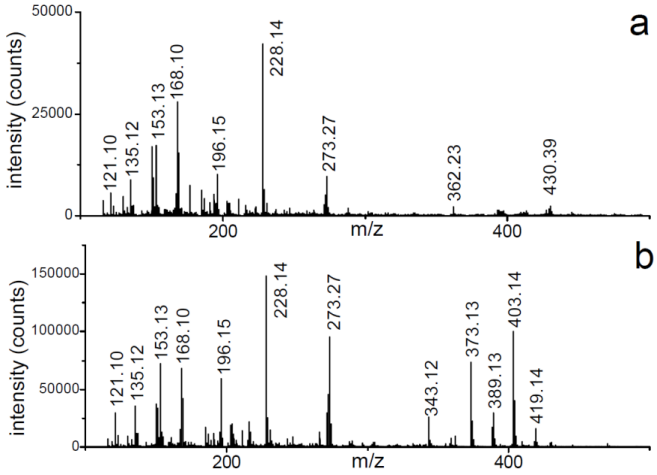

Figure 12 LAAPPI mass spectra obtained in the analysis of a *Citrus aurantium* leaf from a) most of the leaf spots and b) a minority of the leaf spots. The solvent background has been subtracted from both spectra. The spray solvent was toluene with a flow rate of 0.5 µL/min.

A typical spectrum measured from the rat brain sections is presented in Figure 13. Abundant ions were detected at *m/z* 368.34, 369.35, 385.35, and 386.35. Most likely they are due to the $[M\text{-}H_2O]^+$, $[MH\text{-}H_2O]^+$, $[M-H]^+$, and $M^{+\cdot}$ ions of cholesterol, which is one of the most abundant lipids in brain tissue. As a reference, a 10 µL sample of 100 µM cholesterol standard prepared in methanol/water (1:1, *v:v*) was analyzed. The standard solution gave abundant fragment ions at *m/z* 368.4 and m/z 369.4 and a weak $[M-H]^+$ ion, but the $M^{+\cdot}$ ion was not detected. As discussed above, the methanol present in the standard solution may suppress the charge-exchange reaction due to proton transfer from the toluene radical cation to methanol (clusters). Since the rat brain sample matrix does not contain methanol, the radical cation of toluene remains in the system, making the charge-exchange reaction with cholesterol possible. In addition to the possible cholesterol species, the brain spectrum (Figure 13) showed ions at *m/z* 540-700. The ions at *m/z* 551.50, 575.49, 577.52, 579.53, and 603.53 could be due to glycerolipid fragments with C16 and C18 fatty acids and 0-2 double bonds, corresponding to triglyceride [MH-fatty acid]$^+$ or diglyceride $[MH\text{-}H_2O]^+$[169] ions. As a reference, LAAPPI analysis of triglyceride tricaprylin standard (10 µL, 100 µM) was carried out. A MH^+ ion was produced, together with an abundant fragment at *m/z* 327.3 due to the loss of one of its fatty acids ($[MH\text{-}CH_3(CH_2)_6COOH]^+$). Comparison with previously determined LAESI rat brain spectra[147] showed that LAAPPI has better ionization efficiency for nonpolar compounds such as cholesterol, while LAESI is able to efficiently ionize phospholipids. Phospholipids were not detected as molecular weight specific ions in LAAPPI. Thus LAAPPI would appear to provide bioanalytical information complementary to that obtained with LAESI.

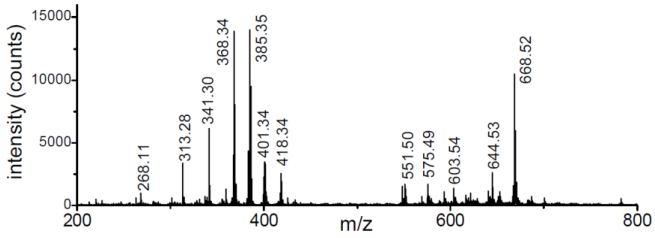

Figure 13 LAAPPI mass spectrum obtained from 200 μm thick section of rat brain with toluene as the spray solvent at a flow rate of 0.5 μL/min.

4.3.2 MASS SPECTROMETRY IMAGING BY LASER ABLATION ATMOSPHERIC PRESSURE PHOTOIONIZATION

The feasibility of LAAPPI for MSI was studied with sage (*Salvia officinalis*) leaves as a tissue model. Sage is a culinary herb but it may also have anti-oxidant[170] and anti-inflammatory properties. The bioactivity of sage has been associated with diterpenes, such as carnosic acid[171] and carnosol,[171] but also may be due to triterpenes, such as ursolic acid found in the plant leaves.[172, 173]

Figure 14 presents a typical LAAPPI spectrum measured from a sage leaf. The spectra were searched for ions that could be due to important sage phytocompounds [170, 171, 173-177] (Table 9). The peaks were attributed to $M^{+\cdot}$, MH^+, and $[M-H]^+$-type ions and/or fragments of the sage phytochemicals. However, the ions could not be fully identified within this study. Absolute identification would require additional MS^n, ion mobility-MS, chromatography-MS, or NMR studies. The obtained data suggest, nevertheless, that LAAPPI-MSI is able to detect volatile compounds, such as monoterpenes (e.g., pinene $M^{+\cdot}$ corresponding to the ion at *m/z* 136.14), and less volatile compounds, possibly carnosic acid ($M^{+\cdot}$ at *m/z* 332.19) and ursolic and/or oleanolic acid ($M^{+\cdot}$ at *m/z* 456.35). Comparison with DAPPI-MSI spectra of sage leaves[99] shows the LAAPPI spectra to contain higher abundance of low molecular weight ions (e.g., mono- and sesquiterpenes). A probable explanation for the difference is that the leaves were dried before the DAPPI analysis, causing the volatile low molecular weight analytes to evaporate. The leaves analysed with LAAPPI were fresh.

MSI images of the spatial distributions of selected ions are presented in Figure 15. The midrib is clearly distinguished from the lamina tissue in the images of the ions at *m/z* 136.14 and 204.20, which may be $M^{+\cdot}$ of mono- and sesquiterpenes, respectively. The distinctive patterns may well reflect the native distribution of the compounds in the tissues, as the sage stems, which serve a similar funtion to the midrib, contain an order of magnitude smaller amount of essential sage oil[176] and only one third the amount of mono- and sesquiterpenes[177] relative to the amounts in the leaves. Note also, however, that the higher tensile strength of the midrib could give it lower ablation efficiency than the lamina tissue, causing it to appear with lower ion intensities.

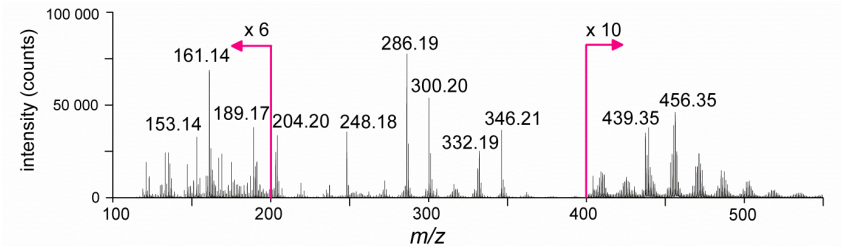

Figure 14 LAAPPI mass spectrum measured from a sage leaf. The solvent background has been subtracted from the spectrum. Note that the m/z 100-200 and 400-550 regions are magnified by factors of 6 and 10, respectively.

The ions at *m/z* 136.14 and 204.20, as well as those at *m/z* 153.14 and 332.19, appear in highest abundance near the tip and close to the edges of the leaf, whereas the ions at *m/z* 136.07 and 456.35 ions are in higher abundance close to the midrib. A comparison with literature (Table 9) suggests that the ions at *m/z* 136.14, 153.14, and 204.20 are due to terpenes and terpenoids of the sage essential oil, while the ion at *m/z* 456.35 may correspond to the radical cation, $M^{+\cdot}$, of ursolic or oleanolic acid (Table 9). Ursolic acid has been associated with the epicuticular wax coating of the leaves of *Salvia blepharophylla*,[178] and the MS image of *m/z* 456.35 ion (Figure 15j) suggests that the wax crystals may be more abundant in the vicinity of the midrib.

Closer study of the spatial location was udertaken by comparing the intensities of the observed ions by correlation analysis methods similar to those applied previously for LAESI-MSI data.[147, 179] High correlation was found between the ions at *m/z* 286.19 and 332.19, suggesting that the former is a fragmentation product of the latter. Similarly, the ion at *m/z* 248.18 is most likely a fragment of the ion(s) at *m/z* 456.35, 455.35, or 439.35, and the ion at *m/z* 316.20 could be due to the rapid air oxdation or photo-oxidation of the species at *m/z* 300.20.

The MSI images and results of the correlation analysis imply that LAAPPI-MSI could be used to study the metabolism of terpenes and terpenoids. In the case of monoterpenes ($M^{+\cdot}$ at *m/z* 136.14) and monoterpenoids (MH^+ at *m/z* 153.14), rapid air or photo-oxidation during sampling is unlikely as the correlation between the ion distributions is relatively weak. More likely, the distributions reflect the local metabolism in the leaf. Camphor offers a second example. The oxidation of camphor (MH^+ corresponding to *m/z* 153.14) to 6-hydroxycamphor (MH^+ possibly at *m/z* 169.13) and further to 6-oxocamphor (MH^+ possibly at *m/z* 167.12) and other metabolites during leaf senescence is a well-known metabolic pathway previously studied in suspension cultures of sage cells.[180] Figure 14k shows that the ions at *m/z* 153.14 and 169.13 are co-localized near the tip of the leaf, where both ions also show highest abundance.

Table 9. *A list of selected abundant ions observed in the LAAPPI-MSI analysis and tentative assignments based on previously reported phytochemicals of Salvia officinalis. The ion marked with * is a possible fragmentation product based on the observed m/z. The two ions marked with ** have been found previously in EI-MS spectra and assigned to fragments of carnosol and carnosic acid, respectively.*[171]

Observed *m/z*	**Phytochemicals reported for sage leaves with possible ions of corresponding *m/z* value**	**Chemical formula**	**Calculated *m/z***	**Δ*m/z***
133.115	p-cymene[177, 181] $[M-H]^+$	$C_{10}H_{13}^+$	133.101	0.014
135.128	p-cymene[177, 181] MH^+	$C_{10}H_{15}^+$	135.117	0.011
	monoterpenes (e.g., α-pinene/β-pinene/limonene/camphene)[176, 177, 181] $[M-H]^+$			
	monoterpenoids (e.g., camphor/α-thujone/β-thujone)[177] $[MH-H_2O]^+$			
136.137	monoterpenes (e.g., α-pinene/β-pinene/limonene/camphene) [176, 177, 181] $M^{+\cdot}$	$C_{10}H_{16}^{+\cdot}$	136.125	0.012
	monoterpenoids (e.g., borneol/1,8-cineole/terpinen-4-ol) [176, 177, 181] $[M-H_2O]^{+\cdot}$			
153.140	monoterpenoids (e.g., borneol/1,8-cineole/terpinen-4-ol) [176, 177, 181] $[M-H]^+$	$C_{10}H_{17}O^+$	153.127	0.013
	monoterpenoids (e.g., camphor/α-thujone/β-thujone/myrtenol) [176, 177, 181] MH^+			
167.119	6-oxocamphor[180] MH^+	$C_{10}H_{15}O_2^+$	167.107	0.013
	6-hydroxycamphor[180] $[M-H]^+$			
169.129	6-hydroxycamphor[180] MH^+	$C_{10}H_{17}O_2^+$	169.122	0.007
203.187	sesquiterpenes (e.g. α-humulene/β-caryophyllene) [176, 177, 181] $[M-H]^+$	$C_{15}H_{23}^+$	203.179	0.008
	caryophyllene oxide[176, 177] $[MH-H_2O]^+$			
204.196	sesquiterpenes (e.g. α-humulene/β-caryophyllene) [176, 177, 181] $M^{+\cdot}$	$C_{15}H_{24}^{+\cdot}$	204.187	0.009
	viridiflorol[176, 177, 181] $[M-H_2O]^{+\cdot}$			
219.173	caryophyllene oxide[176, 177] $[M-H]^+$	$C_{15}H_{23}O^+$	219.174	-0.001
	$[237.189-H_2O]^{+}$*	$C_{15}H_{23}O^+$	219.174	-0.001
272.243	manool[180] $[M-H_2O]^{+\cdot}$	$C_{20}H_{32}^{+\cdot}$	272.250	-0.007
	monoterpenes (e.g. α-pinene/β-pinene/limonene/camphene) [176, 177, 181] $[2M]^{+\cdot}$			
286.187	carnosol $[M-CO_2]^{+\cdot}$ [171] **	$C_{19}H_{26}O_2^{+\cdot}$	286.193	-0.006
	carnosic acid $[M-CO-H_2O]^+$ [171] **			
300.203	dehydroabietic acid[182] $M^{+\cdot}$	$C_{20}H_{28}O_2^{+\cdot}$	300.209	-0.006
	miltirone[183] $[M+NH_4]^+$	$C_{19}H_{26}O_2N^+$	300.196	0.007
316.198	hydroxydehydroabietic acid[182] $M^{+\cdot}$	$C_{20}H_{28}O_3^{+\cdot}$	316.203	0.005
331.190	carnosol[171] MH^+	$C_{20}H_{27}O_4^+$	331.190	0.000
	carnosic acid[171] $[M-H]^+$			
332.188	carnosic acid[171] $M^{+\cdot}$	$C_{20}H_{28}O_4^{+\cdot}$	332.199	-0.011
346.212	12-O-methyl carnosic acid[183] $M^{+\cdot}$	$C_{21}H_{30}O_4^{+\cdot}$	346.214	-0.002
437.341	ursolic acid/oleanolic acid[173] $[M-H-H_2O]^+$	$C_{30}H_{45}O_2^+$	437.341	0.000
439.353	ursolic acid/oleanolic acid[173] $[MH-H_2O]^+$	$C_{30}H_{47}O_2^+$	439.357	-0.004
455.345	ursolic acid/oleanolic acid[173] $[M-H]^+$	$C_{30}H_{47}O_3^+$	455.352	-0.007
456.352	ursolic acid/oleanolic acid[173] $M^{+\cdot}$	$C_{30}H_{48}O_3^{+\cdot}$	456.360	-0.008

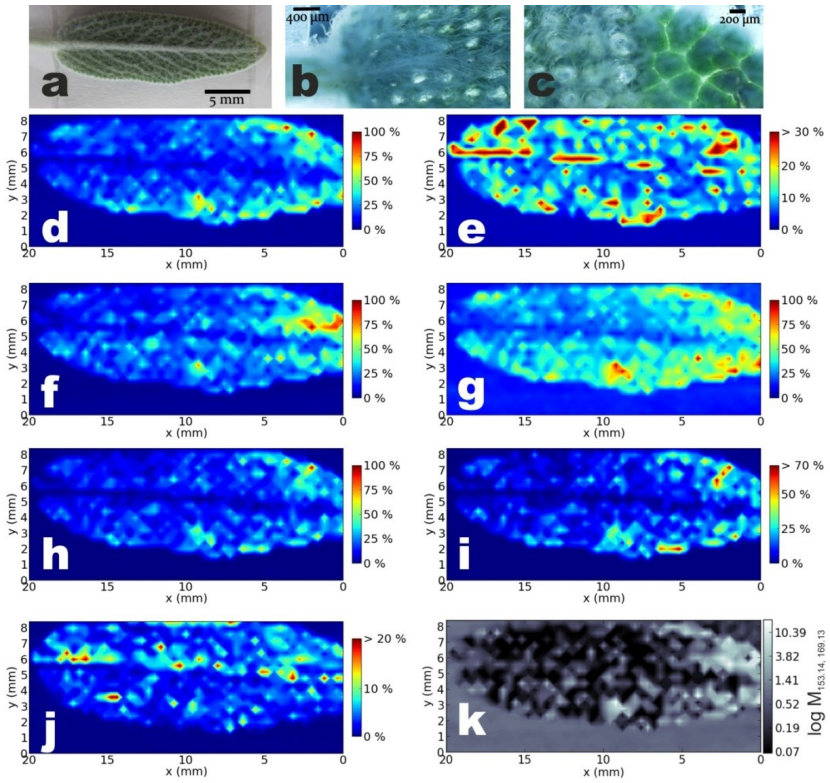

Figure 15 LAAPPI-MSI study of a sage leaf. a) Photograph of the sage leaf before analysis, and post-analysis microscope images of the analyzed sample near b) the petiole, and c) the apex. d-j) Mass spectrometry images showing the spatial distributions of ions at *m/z* d) 136.14, e) 136.07, f) 153.14, g) 169.13, h) 204.20, i) 332.19, and j) 456.35 (normalized to the maximum intensity of each ion). In e), i), and j) the low intensity range was expanded for better visualization (with upper limits of 30, 70, and 20%, respectively). k) Pearson co-localization map of the ions at *m/z* 153.14 and 169.13 (note the logarithmic scale). See Table 9 for previously identified sage phytochemicals possibly corresponding to the studied *m/z* values.

4.4 HEAT-ASSISTED LASER ABLATION ELECTROSPRAY IONIZATION

Modification of the laser ablation electrospray ionization source[38] with a heated gas spray was found to enhance the ionization of neutral and nonpolar compounds enabling more universal ionization compared to conventional LAESI. Study of this observation led to the development of the heat-assisted laser ablation electrospray ion source (HA-LAESI, Figure 4). Only two direct open air sampling/ionization MS sources aiming at universal ionization capabilities have been reported in the literature: DEMI and a combination of DESI and DICE (see Sect. 1.1.5).[45, 46]

Initial HA-LAESI experiments were conducted with a mixture of estrone (a neutral, low polarity compound) and bradykinin 1-8 (a polar peptide) as the sample. No analyte or background signals were detected when the ES emitter voltage was turned off. With the ES emitter voltage on, estrone gave no signal without the gas flow, whereas MH^+ and $[M + 2H]^{2+}$ ions of bradykinin 1–8 were observed even with the gas flow turned off (Figure 16). The effects of the gas temperature and flow rate on the analyte signals were studied by varying the microchip heating power between 0 and 4.0 W (corresponding to jet temperatures from ambient to over 200 °C) and the gas flow rate between 0 and 500 mL/min. Estrone did not produce a signal at heating powers below 2.0 W, but its signal increased as the microchip heating power was increased up to 3.0 W. When the gas flow rate was increased, the signal of estrone grew up to a flow rate of 330 mL/min. Significant changes in the signal of bradykinin 1-8 were not observed in either the heating power or flow rate experiments.

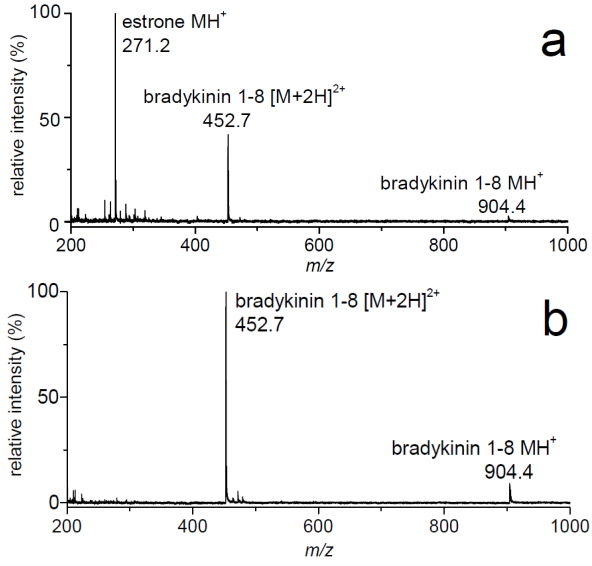

Figure 16 Analysis of a mixture of estrone (25 μM) and bradykinin 1-8 (23 μM) using the HA-LAESI ion source with a) electrospray, N_2 gas flow (180 mL/min) and heating (2.8 W) turned on, and b) electrospray on but N_2 gas flow and heating turned off (LAESI mode). The background has been subtracted from both spectra.

Although these data do not reveal the ionization mechanisms of HA-LAESI, some suggestions can be presented. In TurboIonSpray[184] and Jet Stream sources, heated gas flow enhances the ionization efficiency due to increased evaporation rate[184] and reduced surface tension of the ES droplets.[185] The heated gas flow enhances the signal of both nonpolar[186] and polar compounds.[187-189] Since the solution flow rate in HA-LAESI is much lower (0.4 μL/min) than that applied in TurboIonSpray (5–1000 μL/min) and Jet Stream, the initial droplets should be

significantly smaller in HA-LAESI. Thus it is likely that mechanisms other than increased evaporation and reduced surface tension are involved in HA-LAESI. Perhaps the fusion of the ablated sample projectiles and the ES droplets changes as the droplet size is reduced by the heated gas jet. The hot gas jet might even completely evaporate the sample droplets, leading to secondary electrospray ionization (SESI)[190] of the analytes. SESI-type gas-phase reactions[191, 192] could enhance the ionization of low polarity compounds because the gas-phase proton affinities of many of these compounds are high enough for ionization in the gas phase even if their liquid-phase basicities are too low for electrospray ionization. Presumably, too, the high temperature in HA-LAESI reduces the cluster size of the charged ES and sample solvent species. Since the proton affinities of water and methanol clusters are lower the smaller the cluster,[193-195] reducing the size of the spray solvent (water/methanol 1:1 + 0.1% HCOOH) clusters would improve the gas-phase ionization efficiency of compounds with low proton affinity.

In a next step, several standards (neutral, nonpolar, polar, basic) were diluted in water/methanol (1:1, *v*:*v*) and analyzed by HA-LAESI. Like estrone, many compounds with only a few or no polarizable atoms and no proton-accepting basic groups were protonated in HA-LAESI (e.g., DHEA, tricaprylin, DG(34:1), cholecalciferol). Even the completely nonpolar PAHs perylene and naphtho[2,3-a]pyrene produced MH^+ ions. In addition to MH^+ ions, there were ammonium and sodium adducts (of DHEA, fucose, tricaprylin, and DG(34:1)) and fragments were observed (for cholesterol, DG(34:1), and fucose $[MH-H_2O]^+$, for tricaprylin and DG(34:1) loss of fatty acid chains).

HA-LAESI was also compared with conventional LAESI and LAAPPI (Figure 17). The ionization of the neutral lipids cholesterol, tricaprylin, and DG(34:1) was efficient in HA-LAESI and LAAPPI, whereas conventional LAESI showed only minor peaks for tricaprylin MH^+, $[M+NH_4]^+$, and $[M+Na]^+$ ions. Neutral lipids are typically derivatized before ESI analysis or analyzed by utilizing adduct formation with NH_4^+ ions, for example.[196] Ionization of the polar analyte bradykinin 1–8 was observed with conventional and HA-LAESI sources, while LAAPPI did not show bradykinin 1-8 ions. Additional experiments with other polar molecules, such as fucose and lysozyme, gave similar results. The multiply charged and adduct ion species ($[M+nH]^{n+}$, $[M+NH_4]^+$, and $[M+Na]^+$) observed in HA-LAESI resembled those typically observed in ESI and LAESI and were likely to have formed in electrospray ionization. The compounds not ionized in LAESI but only in HA-LAESI may have ionized through gas-phase ion/molecule reactions.

The quantitative performance of HA-LAESI was evaluated by studying the linearity of the signal of verapamil and determining LODs for estrone, bradykinin 1–8, and verapamil. The linearity was adequate over three decades (n = 11, r^2 = 0.988), and the average relative standard deviation for three sample droplets over the whole concentration range (n = 11) was 22%. The performance was thus semiquantitative. The analysis of 0.5 µL sample droplets showed LODs (determined as amount giving S/N≥3 in time-resolved ion intensity graphs) of 3, 1.2, and 0.13 pmol for estrone, bradykinin 1–8, and verapamil, respectively. Conventional LAESI gave LOD of 0.6 pmol for bradykinin 1-8, which is slightly better than that obtained

with HA-LAESI (1.2 pmol). The poorer result in HA-LAESI may have been due to the elevated temperature of the HA-LAESI ion source, which could induce fragmentation of the peptide, or it may have been due to the different ion source geometry. The LOD obtained for estrone by HA-LAESI was similar to that obtained with LAAPPI (3 pmol, $M^{+\cdot}$ ion), and the LOD obtained for verapamil by HA-LAESI (250 nM) was similar to the LODs obtained previously by conventional LAESI (236 nM)[38] and LAAPPI (250 nm) (III). The LODs determined here for bradykinin 1-8 and estrone by HA-LAESI are ~two orders of magnitude lower than those determined for angiotensin I and dibromodibenzosuberone by DEMI,[45] which is another ambient MS technique capable of ionizing both polar and nonpolar compounds.

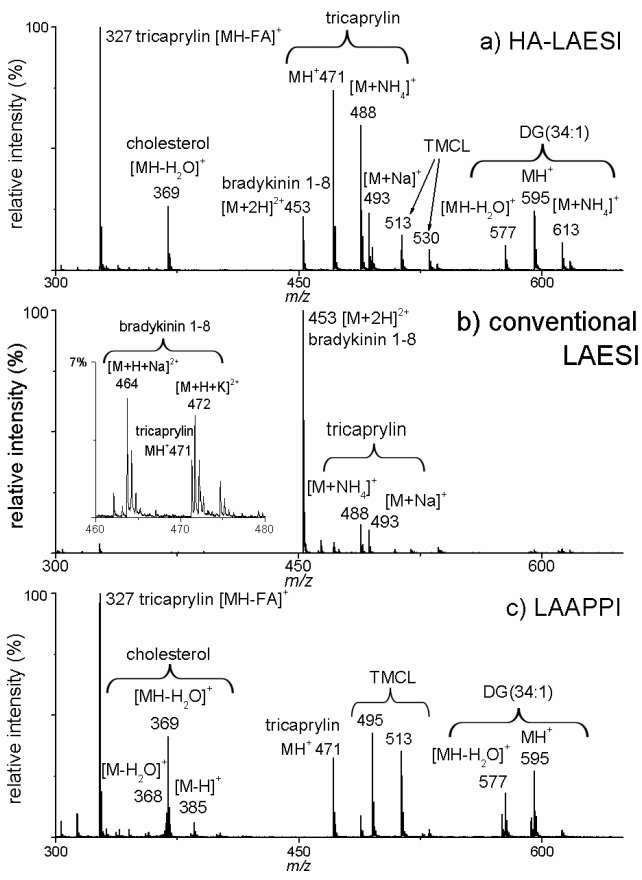

Figure 17 Spectra of a 10 µL droplet of a mixture of tricaprylin (100 µM), tetramyristoyl cardiolipin (TMCL, 100 µM), cholesterol (100 µM), bradykinin 1−8 (92 µM), and 1-palmitoyl-2-oleoyl-sn-glycerol (DG(34:1), 100 µM) obtained by a) HA-LAESI, b) conventional LAESI, and c) LAAPPI. The solvent background has been subtracted from each spectrum.

Applications

Avocado (*Persea americana*) fruit, mouse brain, and pansy (*Viola*) petals were studied to demonstrate the performance of HA-LAESI in real applications. Figure 17a shows the HA-LAESI spectrum recorded from a 0.5 mm thick section of avocado. The most abundant ions most likely correspond to MH^+, $[M+NH_4]^+$, and $[M+Na]^+$ ions of triglycerides (TGs) previously determined in avocado oil.[197, 198] Conventional LAESI of the same fruit showed only minor peaks for ions with *m/z* values corresponding to TG ions (Figure 17b). The result clearly indicates that HA-LAESI has significantly better ionization efficiency than conventional LAESI for nonpolar compounds.

The HA-LAESI analysis of 40 μm thick tissue section from mouse brain showed *m/z* 369.349 as the base peak and other abundant ions at *m/z* range 500-700 (Figure 18). The *m/z* 369.349 ion is most likely due to nonpolar cholesterol $[MH-H_2O]^+$, while the ions at *m/z* 500-700 could be due to neutral lipids (e.g, diglycerides). Cholesterol is one of the most abundant lipids in brain tissue, and HA-LAESI provides better ionization efficiency for the nonpolar lipid than reported for conventional LAESI analysis of rat and mouse brain.[147, 199]

Finally, HA-LAESI-MSI was demonstrated by studying the pigments of pansy (*Viola*) petals. The MSI image of the ion at *m/z* 919.3 (tentatively identified as delphinidin-3-p-coumaroylrhamnosylglucoside-5-glucoside) is shown in Figure 19.

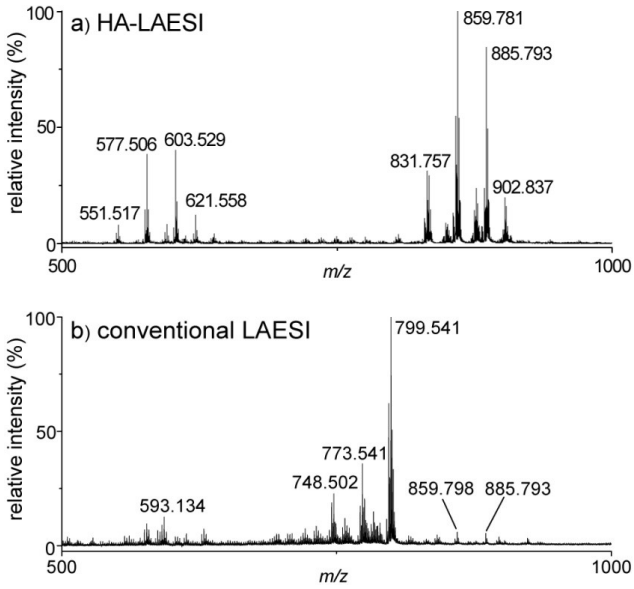

Figure 18 Spectra of avocado fruit pulp section (thickness 0.5 mm) obtained by a) HA-LAESI and b) conventional LAESI.

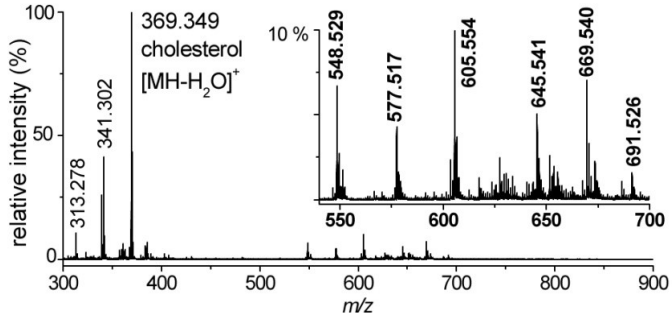

Figure 19 Typical HA-LAESI spectrum of 40 µm thick section of mouse brain.

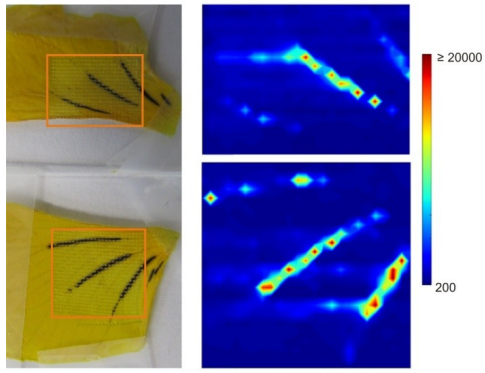

Figure 20 Photograph of pansy petal and spatial distribution of the ion at *m/z* 919.3 measured with conventional LAESI (top, plot size 9.6 × 6.8 mm) and HA-LAESI (bottom, plot size 9.6 × 9.2 mm). The orange squares superimposed on the photo show the approximate areas studied and corresponding to the 2D contour plots. The sample was cooled to ~2 °C on a Peltier cooling stage in an attempt to avoid dehydration of the tissue during the experiment. The sampling step size was 0.4 mm and dwell time 8 s.

5 SUMMARY AND CONCLUSIONS

The aim of the research summarized in this thesis was to develop and apply direct open air surface sampling/ionization mass spectrometry methods suitable for the study of neutral and nonpolar compounds. It was shown in study I that an rf alternating current UV photoionization lamp offers significantly higher ionization efficiency than a direct current lamp with solvents that have high IE (above 10 eV). Measurement of emission spectra of the lamps indicated that the better performance of the rf lamp is due to its higher photon emission. As was demonstrated with μAPPI and DAPPI, ionization techniques relying on photoionization can benefit from the use of the rf lamp. Even completely solvent-free DAPPI is feasible, enabling reduced operating costs, a more environmentally friendly source, and a simpler combination with portable mass spectrometers. In general, it was shown that a comprehensive optimization of the intensity and beam shape of the photoionization lamp could improve APPI applications using low IE solvents, such as those commonly used in reversed-phase LC.

An extraction method for DAPPI-MS analysis of neutral and nonpolar compounds in aqueous samples was developed in study II. PDMS swelled with toluene was used as the extraction material, and the extracted compounds were analyzed by DAPPI-MS directly on the PDMS. The method was shown to overcome most severe matrix effects affecting the DAPPI-MS analysis. As also observed earlier, the selectivity could be tuned by proper choice of the DAPPI spray solvent, but also by choice of the PDMS swelling agent. The method is suited for extraction and *in situ* analysis of medium polar and nonpolar analytes in aqueous samples (e.g., for monitoring of wastewater streams), but the extraction equilibrium time is too long for applications where the results are needed immediately. The extraction could probably be speeded up by optimizing the sorbent material, for example by increasing the ratio of surface area to volume or by selecting another sorbent material. Other extraction methods, such as single-drop microextraction or solid-phase extraction on a pipet tip, might also provide more rapid analyses.

The direct open air surface sampling/ionization MSI of neutral and nonpolar compounds has been limited by either poor sensitivity or low spatial resolution. In remedy of this, a new LAAPPI method with both good sensitivity and spatial resolution was developed in study III. Mid-IR laser ablation was applied to sample spots of approx. 300 μm diameter, and the rf krypton discharge lamp was used for the ionization. Analytes with low IE could be ionized via charge exchange when a suitable spray solvent (e.g., toluene or anisole) was chosen. The approach enabled the detection of neutral and nonpolar compounds which, because of their low proton affinities, cannot be efficiently ionized by proton transfer in either DESI or LAESI. Application of LAAPPI in the fingerprinting and MSI of tissues was also demonstrated. In IV, for example, it was used to get information on the spatial distribution of sage leaf phytochemicals, which are typically analyzed by GC- and LC-MS. The ability to detect neutral and nonpolar analytes makes LAAPPI-MSI a

complementary technique to MALDI, DESI, and LAESI imaging. More work is needed to improve the spatial resolution, but studies on LAESI suggest that at least cell-by-cell level could be achieved with the applied laser. The resolution could be improved by better laser focusing—through the use of thin, sharp optical fiber tips or aspherical lenses, for example. Also, precision of the laser ablation might be improved by using a shorter, femtosecond pulse laser instead of the typically applied nanosecond lasers.

As reported in publication V, simultaneous ionization of nonpolar and polar analytes of diverse sizes was achieved in LAESI by intercepting the electrospray and sample plumes with a heated gas jet. The improved ionization efficiency for low polarity analytes was attributed to enhanced evaporation of solvent from the electrospray and sample droplets and to a mechanism resembling secondary electrospray ionization that allows ionization of low polarity compounds in the gas phase. The HA-LAESI method was demonstrated in the direct analysis of neutral and polar compounds in plant and animal tissues. Compounds of a wider range of polarities than in conventional LAESI or LAAPPI were successfully ionized. More detailed studies are needed to establish the HA-LAESI ionization mechanism and, as in the case of LAAPPI, the spatial resolution of HA-LAESI needs to be improved.

The field of direct open air surface sampling/ionization mass spectrometry has expanded rapidly since the introduction of DESI in 2004. As also seen in the studies of this thesis, the modification of existing and development of new methods has brought improvement in source performance in critical areas such as spatial resolution, ionization efficiency, and sensitivity to different types of compounds. There are now many different techniques capable of similar tasks and it is time for a comprehensive comparison and critical evaluation of sources to establish whether all are really needed. For example, the design of many of the recent techniques like HA-LAESI is complex compared to DESI and DART, and their use may thus not be as easy. However, the more complex techniques can outperform DESI and DART in demanding applications, e.g., when ionization of both polar and nonpolar compounds is necessary or excellent spatial resolution is called for.

Nevertheless, direct open air surface sampling/ionization mass spectrometry is carving out a niche in rapid screening and fingerprinting and is replacing qualitative LC- and GC-MS analyses that do not require ultimate sensitivity but suffer from tedious and lengthy sample preparation procedures. The lower sensitivity, susceptibility to matrix effects, and scarce validation data relevant to quantitative performance limit competitiveness with the more challenging LC- and GC-MS applications. Thus, much more work will be needed before the new techniques are ready to challenge established ones. One feasible strategy would be to develop sample preparation and separation methods compatible with direct open air surface sampling/ionization MS, focusing on the simplification and acceleration of solid-phase extraction, liquid-liquid extraction, and LC separations. Another approach would be hyphenation with existing rapid separation solutions, such as ion and differential mobility cells.

The capabilities of many direct open air surface sampling/ionization MS methods have been demonstrated in the MSI field. In the present work, this was

done for LAAPPI and HA-LAESI. Most ambient MSI work has focused on small basic pharmaceuticals and phospholipids of mammal tissues, perhaps because of their efficient ionization in ESI. Many applications, however, await straightforward strategies and methods for the detection of compounds such as proteins, peptides, and neutral and nonpolar lipids. The alternative methods, including LAAPPI and HA-LAESI, need to be applied in practice for confidence to be gained in their performance. Moreover, before direct open air surface sampling/ionization MSI can be fully established as a reliable alternative to MALDI and SIMS MSI, thorough validation will be needed, especially in regard to possible matrix effects, robustness, and quantitative performance. The spatial resolution also needs to be further improved in order to reach sub-cellular level. Finally, the direct open air surface sampling/ionization MS methods offer novel opportunities in *in vivo* work and so hold great promise in the study of biological problems. Potentially, completely new information could be obtained in cell-level biology.

REFERENCES

1 Gohlke, R. S.; McLafferty, F. W. J. Am. Soc. Mass Spectrom. 1993, 4, 367-371.
2 Munson, M. S. B.; Field, F. H. J. Am. Chem. Soc. 1966, 88, 2621-2630.
3 Tal'roze, V. L.; Ljubimova, A. K. reprint in J. Mass Spectrom. 1998, 33, 502-504.
4 Horning, E. C.; Horning, M. G.; Carroll, D. I.; Dzidic, I.; Stillwell, R. N. Anal.Chem. 1973, 45, 936-943.
5 Tanaka, K.; Waki, H.; Ido, Y.; Akita, S.; Yoshida, Y.; Yohida, T. Rapid Commun. Mass Spectrom. 1988, 2, 151-153.
6 Karas, M.; Bachmann, D.; Bahr, U.; Hillenkamp, F. Int. J. Mass Spectrom. Ion Proces. 1987, 78, 53-68.
7 Karas, M.; Hillenkamp, F. Anal. Chem. 1988, 60, 2299-2301.
8 Dole, M.; Mack, L. L.; Hines, R. L.; Mobley, R. C.; Ferguson, L. D.; Alice, M. B. J. Chem. Phys. 1968, 49, 2240-2249.
9 Yamashita, M.; Fenn, J. B. J. Phys. Chem. 1984, 88, 4451-4459.
10 Fenn, J. B.; Mann, M.; Meng, C. K.; Wong, S. F.; Whitehouse, C. M. Science. 1989, 246, 64-71.
11 Syage, J. A.; Evans, M. D.; Hanold, K. A. Am. Lab. 2000, 32, 24-29.
12 Robb, D. B.; Covey, T. R.; Bruins, A. P. Anal. Chem. 2000, 72, 3653-3659.
13 Tsuchiya, M.; Kuwabara, H. Anal. Chem. 1984, 56, 14-19.
14 Laiko, V. V.; Baldwin, M. A.; Burlingame, A. L. Anal. Chem. 2000, 72, 652-657.
15 Van Berkel, G. J.; Sanchez, A. D.; Quirke, J. M. E. Anal. Chem. 2002, 74, 6216-6223.
16 Coon, J. J.; Steele, H. A.; Laipis, P. J.; Harrison, W. W. J. Mass Spectrom. 2002, 37, 1163-1167.
17 Takáts, Z.; Wiseman, J. M.; Gologan, B.; Cooks, R. G. Science. 2004, 306, 471-473.
18 Cody, R. B.; Laramee, J. A.; Durst, H. D. Anal. Chem. 2005, 77, 2297-2302.
19 Cooks, R. G.; Ouyang, Z.; Takats, Z.; Wiseman, J. M. Science. 2006, 311, 1566-1570.
20 Monge, M. E.; Harris, G. A.; Dwivedi, P.; Fernández, F. M. Chem. Rev. 2013, 113, 2269-2308
21 Van Berkel, G. J.; Pasilis, S. P.; Ovchinnikova, O. J. Mass Spectrom. 2008, 43, 1161-1180.
22 Takáts, Z.; Wiseman, J. M.; Cooks, R. G. J. of Mass Spectrom. 2005, 40, 1261-1275.
23 Venter, A.; Sojka, P. E.; Cooks, R. G. Anal. Chem. 2006, 78, 8549-8555.
24 Costa, A. B.; Cooks, R. G. Chem.Commun. 2007, 3915-3917.
25 Iribarne, J. V.; Thomson, B. A. J. Chem. Phys. 1976, 64, 2287-2294.
26 Badu-Tawiah, A.; Bland, C.; Campbell, D. I.; Cooks, R. G. J. Am. Soc. Mass Spectrom. 2010, 21, 572-579
27 Kauppila, T. J.; Talaty, N.; Kuuranne, T.; Kotiaho, T.; Kostiainen, R.; Cooks, R. G. Analyst. 2007, 132, 868-875.
28 Chen, H.; Cotte-Rodríguez, I.; Cooks, R. G. Chem. Commun. 2006, 6, 597-599.
29 Huang, G.; Chen, H.; Zhang, X.; Cooks, R. G.; Ouyang, Z. Anal. Chem. 2007, 79, 8327-8332.
30 Chan, C.; Bolgar, M. S.; Miller, S. A.; Attygalle, A. B. J.Am.Soc.Mass Spectrom. 2010, 21, 1554-1560.
31 Chen, H.; Ouyang, Z.; Cooks, R. G. Angew. Chem. Int. Ed. 2006, 45, 3656-3660.
32 Ebejer, K. A.; Brereton, R. G.; Carter, J. F.; Ollerton, S. L.; Sleeman, R. Rapid Commun. Mass Spectrom. 2005, 19, 2137-2143.
33 Takáts, Z.; Cotte-Rodriguez, I.; Talaty, N.; Chen, H.; Cooks, R. G. Chem. Commun. 2005, 1950-1952.
34 McEwen, C. N.; McKay, R. G.; Larsen, B. S. Anal. Chem. 2005, 77, 7826-7831.
35 Haapala, M.; Pól, J.; Saarela, V.; Arvola, V.; Kotiaho, T.; Ketola, R. A.; Franssila, S.; Kauppila, T. J.; Kostiainen, R. Anal. Chem. 2007, 79, 7867-7872.
36 Galhena, A. S.; Harris, G. A.; Nyadong, L.; Murray, K. K.; Fernández, F. M. Anal. Chem. 2010, 82, 2178-2181.
37 Shiea, J.; Huang, M.; Hsu, H.; Lee, C.; Yuan, C.; Beech, I.; Sunner, J. Rapid Commun. Mass Spectrom. 2005, 19, 3701-3704.

38 Nemes, P.; Vertes, A. Anal. Chem. 2007, 79, 8098-8106.
39 Sampson, J. S.; Hawkridge, A. M.; Muddiman, D. C. J.Am.Soc.Mass Spectrom. 2006, 17, 1712-1716.
40 Shelley, J. T.; Ray, S. J.; Hieftje, G. M. Anal. Chem. 2008, 80, 8308-8313.
41 Cheng, S.; Cheng, T.; Chang, H.; Shiea, J. Anal. Chem. 2009, 81, 868-874.
42 Ratcliffe, L. V.; Rutten, F. J. M.; Barrett, D. A.; Whitmore, T.; Seymour, D.; Greenwood, C.; Aranda-Gonzalvo, Y.; Robinson, S.; McCoustra, M. Anal. Chem. 2007, 79, 6094-6101.
43 Haddad, R.; Sparrapan, R.; Eberlin, M. N. Rapid Commun. Mass Spectrom. 2006, 20, 2901-2905.
44 Hiraoka, K.; Nishidate, K.; Mori, K.; Asakawa, D.; Suzuki, S. Rapid Commun. Mass Spectrom. 2007, 21, 3139-3144.
45 Nyadong, L.; Galhena, A. S.; Fernández, F. M. Anal. Chem. 2009, 81, 7788-7794.
46 Chan, C.; Bolgar, M. S.; Miller, S. A.; Attygalle, A. B. J. Am. Soc. Mass Spectrom. 2011, 22, 173-178.
47 Cody, R. B. Anal. Chem. 2009, 81, 1101-1107.
48 Vaclavik, L.; Rosmus, J.; Popping, B.; Hajslova, J. J. Chromatogr A. 2010, 1217, 4204-4211.
49 Maleknia, S. D.; Vail, T. M.; Cody, R. B.; Sparkman, D. O.; Bell, T. L.; Adams, M. A. Rapid Commun. Mass Spectrom. 2009, 23, 2241-2246.
50 Vaclavik, L.; Cajka, T.; Hrbek, V.; Hajslova, J. Anal. Chim. Acta. 2009, 645, 56-63.
51 Yu, S.; Crawford, E.; Tice, J.; Musselman, B.; Wu, J. Anal. Chem. 2009, 81, 193-202.
52 Saang'onyo, D. S.; Smith, D. L. Rapid Commun. Mass Spectrom. 2012, 26, 385-391.
53 Zhao, Y.; Lam, M.; Wu, D.; Mak, R. Rapid Commun. Mass Spectrom. 2008, 22, 3217-3224.
54 Harris, G. A.; Fernández, F. M. Anal. Chem. 2009, 81, 322-329.
55 Song, L.; Gibson, S. C.; Bhandari, D.; Cook, K. D.; Bartmess, J. E. Anal. Chem. 2009, 81, 10080-10088.
56 Domin, M. A.; Steinberg, B. D.; Quimby, J. M.; Smith, N. J.; Greene, A. K.; Scott, L. T. Analyst. 2010, 135, 700-704.
57 Cotte-Rodríguez, I.; Takáts, Z.; Talaty, N.; Chen, H.; Cooks, R. G. Anal. Chem. 2005, 77, 6755-6764.
58 Williams, J. P.; Scrivens, J. H. Rapid Commun. Mass Spectrom. 2005, 19, 3643-3650.
59 Williams, J. P.; Patel, V. J.; Holland, R.; Scrivens, J. H. Rapid Commun. Mass Spectrom. 2006, 20, 1447-1456.
60 Luosujärvi, L.; Arvola, V.; Haapala, M.; Pól, J.; Saarela, V.; Franssila, S.; Kotiaho, T.; Kostiainen, R.; Kauppila, T. J. Anal. Chem. 2008, 80, 7460-7466.
61 Kauppila, T. J.; Kuuranne, T.; Meurer, E. C.; Eberlin, M. N.; Kotiaho, T.; Kostiainen, R. Anal. Chem. 2002, 74, 5470-5479.
62 NIST Chemistry Webbook, http://webbook.nist.gov/chemistry/
63 Luosujärvi, L.; Kanerva, S.; Saarela, V.; Franssila, S.; Kostiainen, R.; Kotiaho, T.; Kauppila, T. J. Rapid Commun. Mass Spectrom. 2010, 24, 1-8.
64 Robb, D. B.; Smith, D. R.; Blades, M. W. J. Am. Soc. Mass Spectrom. 2008, 19, 955-963.
65 Syage, J. A. J. Am. Soc. Mass Spectrom. 2004, 15, 1521-1533.
66 Robb, D. B.; Blades, M. W. J. Am. Soc. Mass Spectrom. 2005, 16, 1275-1290.
67 Itoh, N.; Aoyagi, Y.; Yarita, T. J.Chromatogr.A. 2006, 1131, 285-288.
68 Suni, N. M.; Aalto, H.; Kauppila, T. J.; Kotiaho, T.; Kostiainen, R. J. Mass. Spectrom. 2012, 47, 611–619.
69 Kauppila, T. J.; Kotiaho, T.; Kostiainen, R.; Bruins, A. P. J. Am. Soc. Mass Spectrom. 2004, 15, 203-211.
70 Basso, E.; Marotta, E.; Seraglia, R.; La Tubaro, M.; Traldi, P. J. Mass Spectrom. 2003, 38, 1113-1115.
71 Song, L.; Wellman, A. D.; Yao, H.; Adcock, J. Rapid Commun. Mass Spectrom. 2007, 21, 1343-1351.
72 Song, L.; Wellman, A. D.; Yao, H.; Bartmess, J. E. J. Am. Soc. Mass Spectrom. 2007, 18, 1789-1798.
73 Suni, N. M.; Lindfors, P.; Laine, O.; Östman, P.; Ojanperä, I.; Kotiaho, T.; Kauppila, T. J.; Kostiainen, R. Anal. Chim. Acta. 2011, 699, 73-80.
74 Dreisewerd, K. Chem.Rev. 2003, 103, 395-425.

75 Shori, R. K.; Walston, A. A.; Stafsudd, O. M.; Fried, D.; Walsh Jr., J. T. IEEE J. Sel. Top. Quantum. Electron. 2001, 7, 959-970.
76 Vogel, A.; Venugopalan, V. Chem. Rev. 2003, 103, 577-644.
77 Schwartz, S. A.; Reyzer, M. L.; Caprioli, R. M. J. Mass Spectrom. 2003, 38, 699-708.
78 Karas, M.; Bachmann, D.; Hillenkamp, F. Anal. Chem. 1985, 57, 2935-2939.
79 Hölscher, D.; Shroff, R.; Knop, K.; Gottschaldt, M.; Crecelius, A.; Schneider, B.; Heckel, D. G.; Schubert, U. S.; Svatoš, A. Plant J. 2009, 60, 907-918.
80 Jorabchi, K.; Hanold, K.; Syage, J. Anal. Bioanal.Chem. 2012, DOI 10.1007/s00216-012-6536-z.
81 Chen, H.; Talaty, N. N.; Takáts, Z.; Cooks, R. G. Anal. Chem. 2005, 77, 6915-6927.
82 Nyadong, L.; Late, S.; Green, M. D.; Banga, A.; Fernández, F. M. J. Am. Soc. Mass Spectrom. 2008, 19, 380-388.
83 Luosujärvi, L.; Laakkonen, U.; Kostiainen, R.; Kotiaho, T.; Kauppila, T. J. Rapid Commun. Mass Spectrom. 2009, 23, 1401-1404.
84 Talaty, N.; Mulligan, C. C.; Justes, D. R.; Jackson, A. U.; Noll, R. J.; Cooks, R. G. Analyst. 2008, 133, 1532-1540.
85 Petucci, C.; Diffendal, J.; Kaufman, D.; Mekonnen, B.; Terefenko, G.; Musselman, B. Anal. Chem. 2007, 79, 5064-5070.
86 Abdelnur, P. V.; Eberlin, L. S.; De Sá, G. F.; De Souza, V.; Eberlin, M. N. Anal. Chem. 2008, 80, 7882-7886.
87 Nefliu, M.; Venter, A.; Cooks, R. G. Chem.Commun. 2006, 888-890.
88 Dane, A. J.; Cody, R. B. Analyst. 2010, 135, 696-699.
89 Nemes, P.; Barton, A. A.; Li, Y.; Vertes, A. Anal. Chem. 2008, 80, 4575-4582.
90 Schäfer, K.; Dénes, J.; Albrecht, K.; Szaniszló, T.; Balogh, J.; Skoumal, R.; Katona, M.; Tóth, M.; Balogh, L.; Takáts, Z. Angew. Chem. Int. Ed. 2009, 48, 8240-8242.
91 Shrestha, B.; Patt, J. M.; Vertes, A. Anal. Chem. 2011, 83, 2947-2955.
92 Yew, J. Y.; Cody, R. B.; Kravitz, E. A. PNAS. 2008, 105, 7135-7140.
93 Wiseman, J. M.; Puolitaival, S. M.; Takáts, Z.; Cooks, R. G.; Caprioli, R. M. Angew. Chem. Int. Ed. 2005, 44, 7094-7097.
94 Ifa, D. R.; Jackson, A. U.; Paglia, G.; Cooks, R. G. Anal. Bioanal. Chem. 2009, 394, 1995-2008.
95 Harris, G. A.; Galhena, A. S.; Fernandez, F. M. Anal. Chem. 2011, 83, 4508-4538.
96 Nyadong, L.; Quinn, J. P.; Hsu, C. S.; Hendrickson, C. L.; Rodgers, R. P.; Marshall, A. G. Anal. Chem. 2012, 84, 7131-7137.
97 Wu, C.; Qian, K.; Nefliu, M.; Cooks, R. G. J. Am. Soc. Mass Spectrom. 2010, 21, 261-267.
98 Wu, C.; Ifa, D. R.; Manicke, N. E.; Cooks, R. G. Anal. Chem. 2009, 81, 7618-7624.
99 Pól, J.; Vidova, V.; Kruppa, G.; Kobliha, V.; Novak, P.; Lemr, K.; Kotiaho, T.; Kostiainen, R.; Havlicek, V.; Volny, M. Anal. Chem. 2009, 81, 8479-8487.
100 Kauppila, T. J.; Talaty, N.; Jackson, A. U.; Kotiaho, T.; Kostiainen, R.; Cooks, R. G. Chem.Commun. 2008, 2674-2676.
101 Nielen, M. W. F.; Hooijerink, H.; Claassen, F. C.; van Engelen, M. C.; van Beek, T. A. Anal. Chim. Acta. 2009, 637, 92-100.
102 Kauppila, T. J.; Flink, A.; Haapala, M.; Laakkonen, U.-M.; Aalberg, L.; Ketola, R. A.; Kostiainen, R. Forensic Sci. Int. 2011, 210, 206-212.
103 McEwen, C.; Gutteridge, S. J. Am. Soc. Mass Spectrom. 2007, 18, 1274-1278.
104 Eberlin, L. S.; Abdelnur, P. V.; Passero, A.; De Sa, G. F.; Daroda, R. J.; De Souza, V.; Eberlin, M. N. Analyst. 2009, 134, 1652-1657.
105 Alberici, L. C.; Oliveira, H. C.; Catharino, R. R.; Vercesi, A. E.; Eberlin, M. N.; Alberici, R. M. Anal. Bioanal. Chem. 2011, 401, 1651-1659.
106 Funasaki, M.; Oliveira, R. S.; Zanotto, S. P.; Carioca, C. R. F.; Simas, R. C.; Eberlin, M. N.; Alberici, R. M. J. Agric. Food Chem. 2012, 60, 11263-11267.
107 Gerbig, S.; Takáts, Z. Rapid Commun. Mass Spectrom. 2010, 24, 2186-2192.
108 Girod, M.; Shi, Y.; Cheng, J.; Cooks, R. G. Anal. Chem. 2011, 83, 207-215.
109 Rummel, J. L.; McKenna, A. M.; Marshall, A. G.; Eyler, J. R.; Powell, D. H. Rapid Commun. Mass Spectrom. 2010, 24, 784-790.
110 Benassi, M.; Berisha, A.; Romão, W.; Babayev, E.; Römpp, A.; Spengler, B. Rapid Commun. Mass Spectrom. 2013, 27, 825--834.
111 Vaclavik, L.; Zachariasova, M.; Hrbek, V.; Hajslova, J. Talanta. 2010, 82, 1950-1957.
112 Ackerman, L. K.; Noonan, G. O.; Begley, T. H. Food Addit. Contam. Part A Chem. Anal. Control Exposure Risk Assess. 2009, 26, 1611-1618.

113 Rothenbacher, T.; Schwack, W. Rapid Commun. Mass Spectrom. 2010, 24, 21-29.
114 Rothenbacher, T.; Schwack, W. Rapid Commun. Mass Spectrom. 2009, 23, 2829-2835.
115 Haefliger, O. P.; Jeckelmann, N. Rapid Commun. Mass Spectrom. 2007, 21, 1361-1366.
116 Kauppila, T. J.; Wiseman, J. M.; Ketola, R. A.; Kotiaho, T.; Cooks, R. G.; Kostiainen, R. Rapid Commun. Mass Spectrom. 2006, 20, 387-392.
117 Harris, G. A.; Falcone, C. E.; Fernández, F. M. J. Am. Soc. Mass Spectrom. 2012, 23, 153-161.
118 Nyadong, L.; Hohenstein, E. G.; Johnson, K.; Sherrill, C. D.; Green, M. D.; Fernández, F. M. Analyst. 2008, 133, 1513-1522.
119 Nilles, J. M.; Connell, T. R.; Durst, H. D. Anal. Chem. 2009, 81, 6744-6749.
120 Wiseman, J. M.; Evans, C. A.; Bowen, C. L.; Kennedy, J. H. Analyst. 2010, 135, 720-725.
121 D'Aloise, P.; Chen, H. Sci. Justice. 2012, 52, 2-8.
122 Nielen, M. W. F.; Nijrolder, A. W. J. M.; Hooijerink, H.; Stolker, A. A. M. Anal. Chim. Acta. 2011, 700, 63-69.
123 Basile, F.; Sibray, T.; Belisle, J. T.; Bowen, R. A. Anal. Biochem. 2011, 408, 289-296.
124 Zhou, M.; McDonald, J. F.; Fernández, F. M. J. Am. Soc. Mass Spectrom. 2010, 21, 68-75.
125 Zhou, M.; Guan, W.; Walker, L. D.; Mezencev, R.; Benigno, B. B.; Gray, A.; Fernández, F. M.; McDonald, J. F. Cancer Epidemiol. Biomarkers Prev. 2010, 19, 2262-2271.
126 García-Reyes, J. F.; Jackson, A. U.; Molina-Díaz, A.; Cooks, R. G. Anal. Chem. 2009, 81, 820-829.
127 Thunig, J.; Flø, L.; Pedersen-Bjergaard, S.; Hansen, S. H.; Janfelt, C. Rapid Commun. Mass Spectrom. 2012, 26, 133-140.
128 Paglia, G.; Ifa, D. R.; Wu, C.; Corso, G.; Cooks, R. G. Anal. Chem. 2010, 82, 1744-1750.
129 Van Berkel, G. J.; Tomkins, B. A.; Kertesz, V. Anal. Chem. 2007, 79, 2778-2789.
130 Van Berkel, G. J.; Kertesz, V. Anal. Chem. 2006, 78, 6283-6283.
131 Van Berkel, G. J.; Ford, M. J.; Deibel, M. A. Anal. Chem. 2005, 77, 1207-1215.
132 Morlock, G.; Ueda, Y. J.Chromatogr.A. 2007, 1143, 243-251.
133 Denes, J.; Katona, M.; Hosszu, A.; Czuczy, N.; Takats, Z. Anal. Chem. 2009, 81, 1669-1675.
134 D'Agostino, P. A.; Chenier, C. L.; Hancock, J. R.; Jackson Lepage, C. R. Rapid Commun.Mass Spectrom. 2007, 21, 543-549.
135 Strittmatter, N.; Düring, R.; Takáts, Z. Analyst. 2012, 137, 4037-4044.
136 Mulligan, C. C.; MacMillan, D. K.; Noll, R. J.; Cooks, R. G. Rapid Commun. Mass Spectrom. 2007, 21, 3729-3736.
137 Sun, X.; Miao, Z.; Yuan, Z.; Harrington, P. D. B.; Colla, J.; Chen, H. Int. J. Mass Spectrom. 2011, 301, 102-108.
138 Amstalden van Hove, E. R.; Smith, D. F.; Heeren, R. M. A. J. Chromatogr., A. 2010, 1217, 3946-3954.
139 Caprioli, R. M.; Farmer, T. B.; Gile, J. Anal. Chem. 1997, 69, 4751-4760.
140 Liebl, H. J. Appl. Phys. 1967, 38, 5277-5283.
141 Spengler, B.; Hubert, M. J. Am. Soc. Mass Spectrom. 2002, 13, 735-748.
142 Guerquin-Kern, J.; Wu, T.; Quintana, C.; Croisy, A. BBA-Gen. Subjects. 2005, 1724, 228-238.
143 Ovchinnikova, O. S.; Nikiforov, M. P.; Bradshaw, J. A.; Jesse, S.; Van Berkel, G. J. ACS Nano. 2011, 5, 5526-5531.
144 Wiseman, J. M.; Ifa, D. R.; Song, Q.; Cooks, R. G. Angew. Chem. Int. Ed. 2006, 45, 7188-7192.
145 Wiseman, J. M.; Ifa, D. R.; Zhu, Y.; Kissinger, C. B.; Manicke, N. E.; Kissingera, P. T.; Cooks, R. G. PNAS. 2008, 105, 18120-18125.
146 Campbell, D. I.; Ferreira, C. R.; Eberlin, L. S.; Cooks, R. G. Anal. Bioanal. Chem. 2012, 404, 389-398.
147 Nemes, P.; Woods, A. S.; Vertes, A. Anal. Chem. 2010, 82, 982-988.
148 Huang, M.; Cheng, S.; Jhang, S.; Chou, C.; Cheng, C.; Shiea, J.; Popov, I. A.; Nikolaev, E. N. Int. J. Mass Spectrom. 2012, 325-327, 172-182.
149 Coello, Y.; Daniel Jones, A.; Gunaratne, T. C.; Dantus, M. Anal. Chem. 2010, 82, 2753-2758.
150 Kauppila, T. J.; Östman, P.; Marttila, S.; Ketola, R. A.; Kotiaho, T.; Franssila, S.; Kostiainen, R. Anal. Chem. 2004, 76, 6797-6801.

151 Saarela, V.; Haapala, M.; Kostiainen, R.; Kotiaho, T.; Franssila, S. Lab Chip. 2007, 7, 644-646.
152 Saarela, V.; Haapala, M.; Kostiainen, R.; Kotiaho, T.; Franssila, S. J. Micromech. Microeng. 2009, 19, 055001
153 Short, L. C.; Cai, S.; Syage, J. A. J. Am. Soc. Mass Spectrom. 2007, 18, 589-599.
154 Kauppila, T. J.; Kostiainen, R.; Bruins, A. P. Rapid Commun. Mass Spectrom. 2004, 18, 808-815.
155 Tubaro, M.; Marotta, E.; Seraglia, R.; Traldi, P. Rapid Commun. Mass Spectrom. 2003, 17, 2423-2429.
156 Kostko, O.; Belau, L.; Wilson, K. R.; Ahmed, M. J. Phys. Chem. A. 2008, 112, 9555-9562.
157 Sánchez-Rojas, F.; Bosch-Ojeda, C.; Cano-Pavón, J. M. Chromatographia. 2009, 69
158 Baltussen, E.; Sandra, P.; David, F.; Cramers, C. J.Microcolumn Sep. 1999, 11, 737-747.
159 Lord, H.; Pawliszyn, J. J. Chromatogr. A. 2000, 885, 153-193.
160 Lee, J. N.; Park, C.; Whitesides, G. M. Anal. Chem. 2003, 75, 6544-6554.
161 Syracuse Science Center interactive log Kow DEMO, SRC's LOGKOW/KOWWIN Program, 2010, http://www.syrres.com/what-wedo/databaseforms.aspx?id=385 (accessed 7th of April 2010).
162 Östman, P.; Pakarinen, J. M. H.; Vainiotalo, P.; Franssila, S.; Kostiainen, R.; Kotiaho, T. Rapid Commun. Mass Spectrom. 2006, 20, 3669-3673.
163 Novak, I.; Potts, A. W. BBA-Bioenerg.1997, 1319, 86-90.
164 Bouchonnet, S.; Genty, C.; Bourcier, S.; Sablier, M. Rapid Commun. Mass Spectrom. 2010, 24, 973-978.
165 Lota, M.; De Serra, D. R.; Jacquemond, C.; Tomi, F.; Casanova, J. Flavour Fragrance J. 2001, 16, 89-96.
166 De Pasquale, F.; Siragusa, M.; Abbate, L.; Tusa, N.; De Pasquale, C.; Alonzo, G. Sci. Hortic. 2006, 109, 54-59.
167 Kawaii, S.; Tomono, Y.; Katase, E.; Ogawa, K.; Yano, M.; Koizumi, M.; Ito, C.; Furukawa, H. J. Agric. Food Chem. 2000, 48, 3865-3871.
168 Thomson, W. W.; Platt-Aloian, K. A.; Endress, A. G. Bot. Gazette. 1976, 137, 330.
169 Cai, S.; Syage, J. A. Anal. Chem. 2006, 78, 1191-1199.
170 Suhaj, M. J. Food Compos. Anal. 2006, 19, 531-537.
171 Schwarz, K.; Ternes, W. Z Lebensm Unters Forch. 1992, 195, 99-103.
172 Bolta, Z.; Baričevic,ˇ.; Bohanec, B.; Andrenšek, S. Plant Cell Tissue Organ Cult. 2000, 62, 57-63.
173 Razboršek, M. I.; Vončina, D. B.; Doleček, V.; Vončina, E. Chromatographia. 2008, 67, 433-440.
174 Schwarz, K.; Ternes, W. Z Lebensm Unters Forch. 1992, 195, 95-98.
175 Lu, Y.; Yeap Foo, L. Phytochemistry. 2002, 59, 117-140.
176 Perry, N. B.; Anderson, R. E.; Brennan, N. J.; Douglas, M. H.; Heaney, A. J.; McGimpsey, J. A.; Smallfield, B. M. J. Agric. Food Chem. 1999, 47, 2048-2054.
177 Santos-Gomes, P. C.; Fernandes-Ferreira, M. J. Agric. Food Chem. 2001, 49, 2908-2916.
178 Bisio, A.; Corallo, A.; Gastaldo, P.; Romussi, G.; Ciarallo, G.; Fontana, N.; De Tommasi, N.; Profumo, P. Ann. Bot. 1999, 83, 441-452.
179 Nemes, P.; Barton, A. A.; Vertes, A. Anal. Chem. 2009, 81, 6668-6675.
180 Funk, C.; Koepp, A. E.; Croteau, R. Arch. Biochem. Biophys. 1992, 294, 306-313.
181 Radulescu, V.; Chiliment, S.; Oprea, E. J.Chromatogr.A. 2004, 1027, 121-126.
182 Kivilompolo, M.; Obůrka, V.; Hyötyläinen, T. Anal. Bioanal. Chem. 2007, 388, 881-887.
183 Miura, K.; Kikuzaki, H.; Nakatani, N. Phytochemistry. 2001, 58, 1171-1175.
184 Li, L.; Campbell, D.; Bennett, P.; Henion, J. Anal. Chem. 1996, 68, 3397-3404.
185 Lu, W.; Bennett, B. D.; Rabinowitz, J. D. J.Chromatogr. B. 2008, 871, 236-242.
186 Careri, M.; Elviri, L.; Mangia, A. J. Chromatogr. A. 1999, 854, 233-244.
187 Boscaro, F.; Pieraccini, G.; La Marca, G.; Bartolucci, G.; Luceri, C.; Luceri, F.; Moneti, G. Rapid Commun. Mass Spectrom. 2002, 16, 1507-1514.
188 Hu, C.; Chao, M.; Sie, C. Free Radic. Biol. Med. 2010, 48, 89-97.
189 Ferrer, I.; Thurman, E. M.; Zweigenbaum, J. A. Ultrasensitive EPA Method 1694 with the Agilent 6460 ESI/MS/MS with Het Stream Technology for Pharmaceuticals and Personal Care Products in Water Application Note, 2010, Agilent Technologies.

http://www.chem.agilent.com/library/applications/5990-4605en.pdf.(accessed 7/18/2012)
190 Fernandez De La Mora, J. Int. J. Mass Spectrom. 2011, 300, 182-193.
191 Martinez-Lozano Sinues, P.; Criado, E.; Vidal, G. Int. J. Mass Spectrom. 2012, 313, 21-29.
192 Tam, M.; Hill Jr., H. H. Anal. Chem. 2004, 76, 2741-2747.
193 Knochenmuss, R.; Cheshnovsky, O.; Leutwyler, S. Chem. Phys. Lett. 1988, 144, 317-323.
194 Meot-Ner, M. J. Am. Chem. Soc. 1986, 108, 6189-6197.
195 Grimsrud, E. P.; Kebarle, P. J. Am. Chem. Soc. 1973, 95, 7939-7943.
196 Murphy, R. C.; Fiedler, J.; Hevko, J. Chem. Rev. 2001, 101, 479-526.
197 Lísa, M.; Holčapek, M. J. Chromatogr. A. 2008, 1198-1199, 115-130.
198 Jakab, A.; Héberger, K.; Forgács, E. J. Chromatogr. A. 2002, 976, 255-263.
199 Shrestha, B.; Nemes, P.; Nazarian, J.; Hathout, Y.; Hoffman, E. P.; Vertes, A. Analyst. 2010, 135, 751-758.